Electronic Supplementary Information

A New Approach to the Effects of Isocyanide (CN-R) Ligands on the Luminescence Properties of Cycloplatinated(II) Complexes

Hamid R. Shahsavari,[a] Reza Babadi Aghakhanpour,[a] Mojdeh Hossein-Abadi,[a] Mohsen Golbon Haghighi,[b] Behrouz Notash,[b] and Masood Fereidoonnezhad[c]*

[a]Department of Chemistry, Institute for Advanced Studies in Basic Sciences (IASBS), Yousef Sobouti Blvd., Zanjan 45137-66731, Iran.

[b]Department of Chemistry, Shahid Beheshti University, Evin, Tehran 19839-69411, Iran.

[c]Department of Medicinal Chemistry, School of Pharmacy; Cancer, Environmental and Petroleum Pollutants Research Center, Ahvaz Jundishapur University of Medical Sciences, Ahvaz, Iran.

Email: shahsavari@iasbs.ac.ir

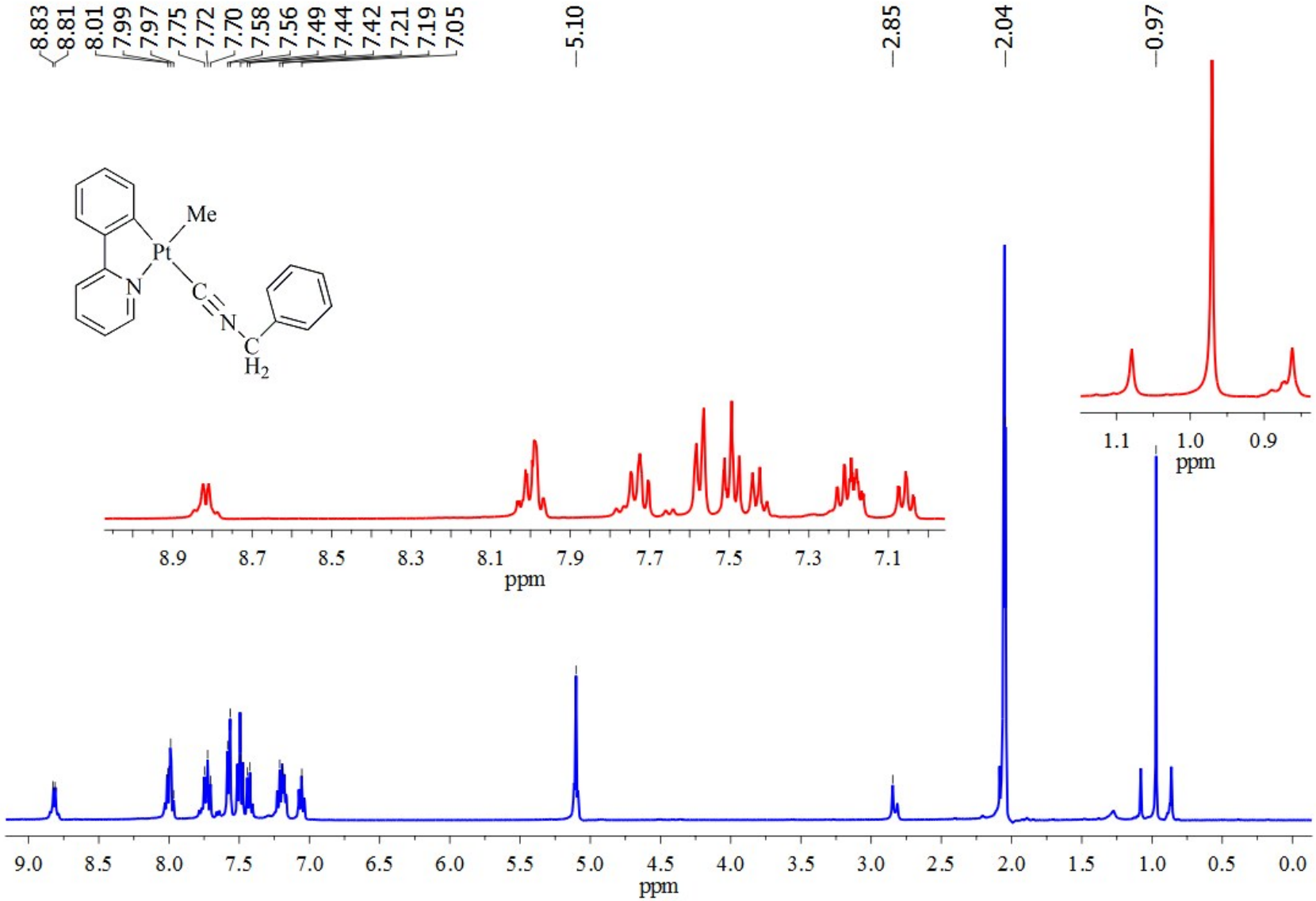

Figure S1. ^{1}HNMR spectrum of [Pt(ppy)(Me)(CN-Bz)], **1**, in acetone d_6.

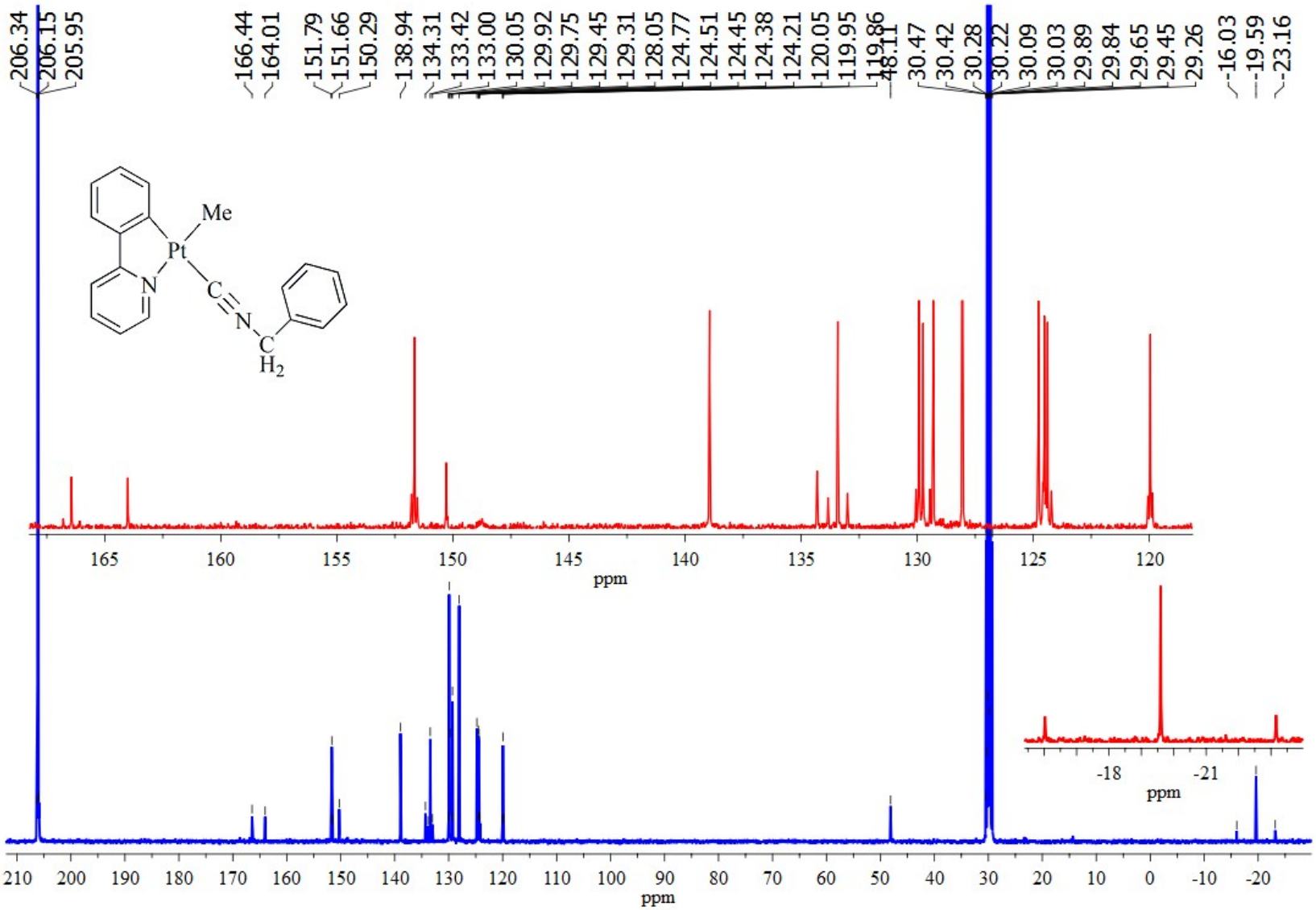

Figure S2. ^{13}CNMR spectrum of [Pt(ppy)(Me)(CN-Bz)], **1**, in acetone d_6.

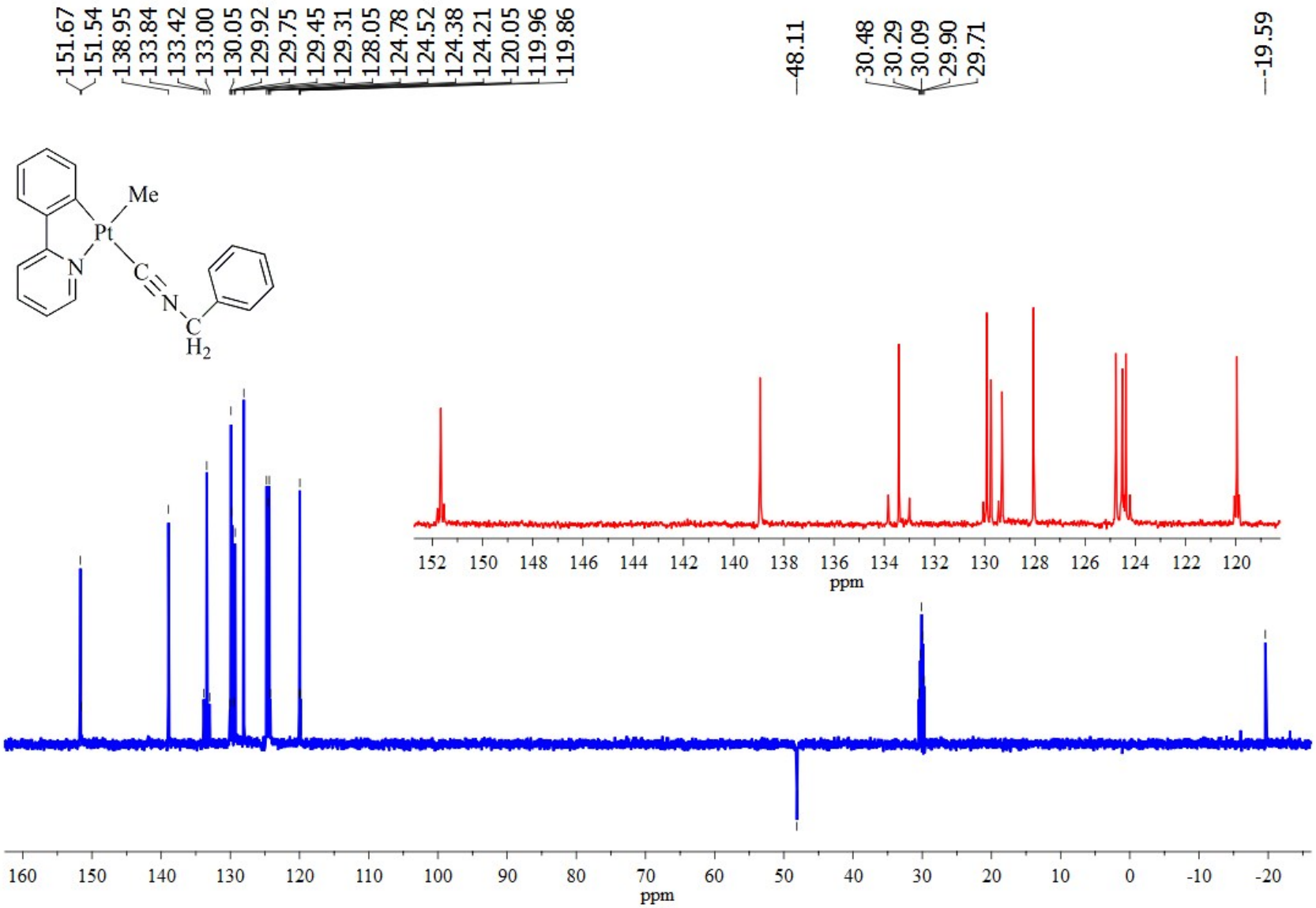

Figure S3. DEPT 135° spectrum of [Pt(ppy)(Me)(CN-Bz)], **1**, in acetone d_6.

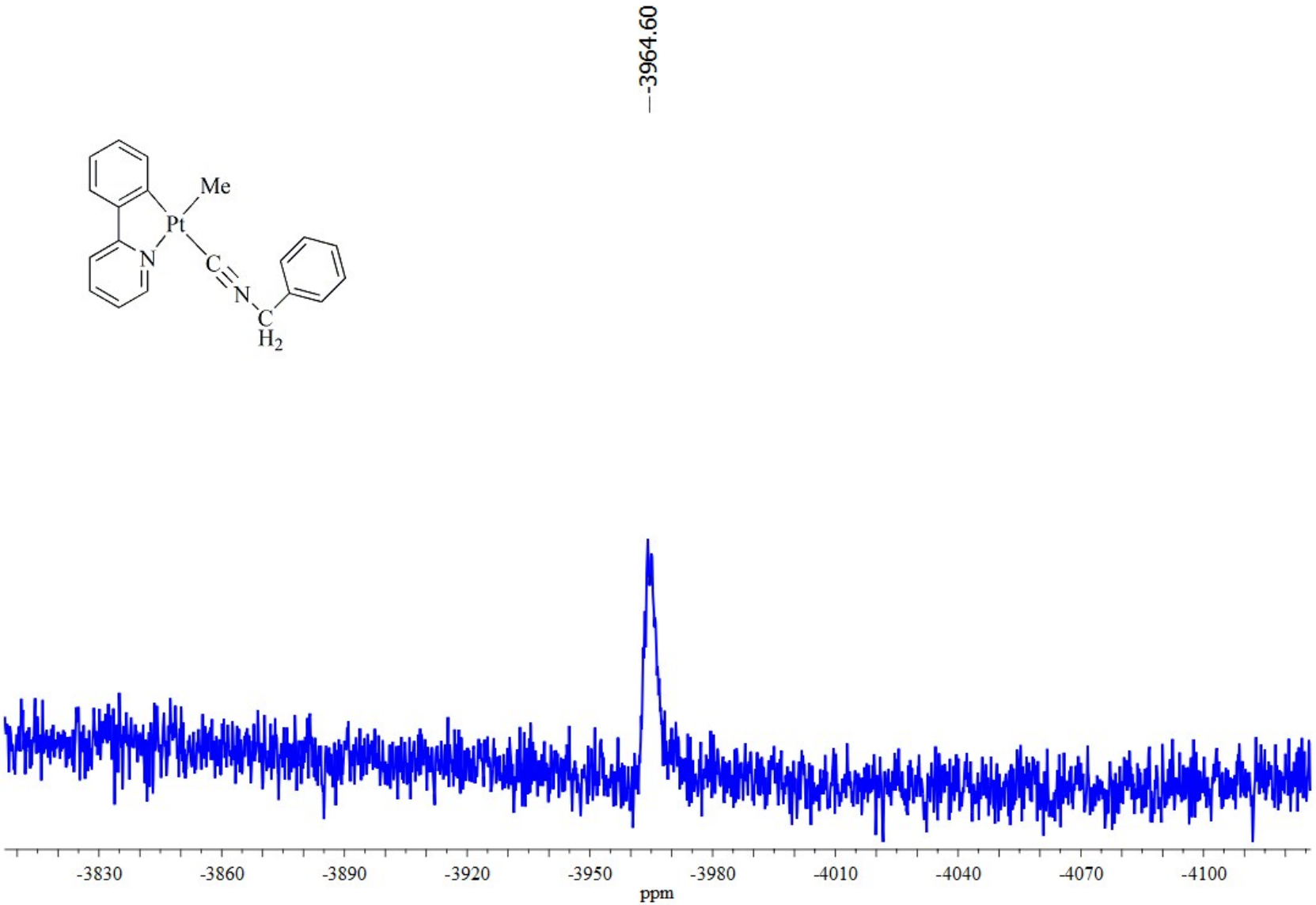

Figure S4. ^{195}PtNMR spectrum of [Pt(ppy)(Me)(CN-Bz)], **1**, in acetone d_6.

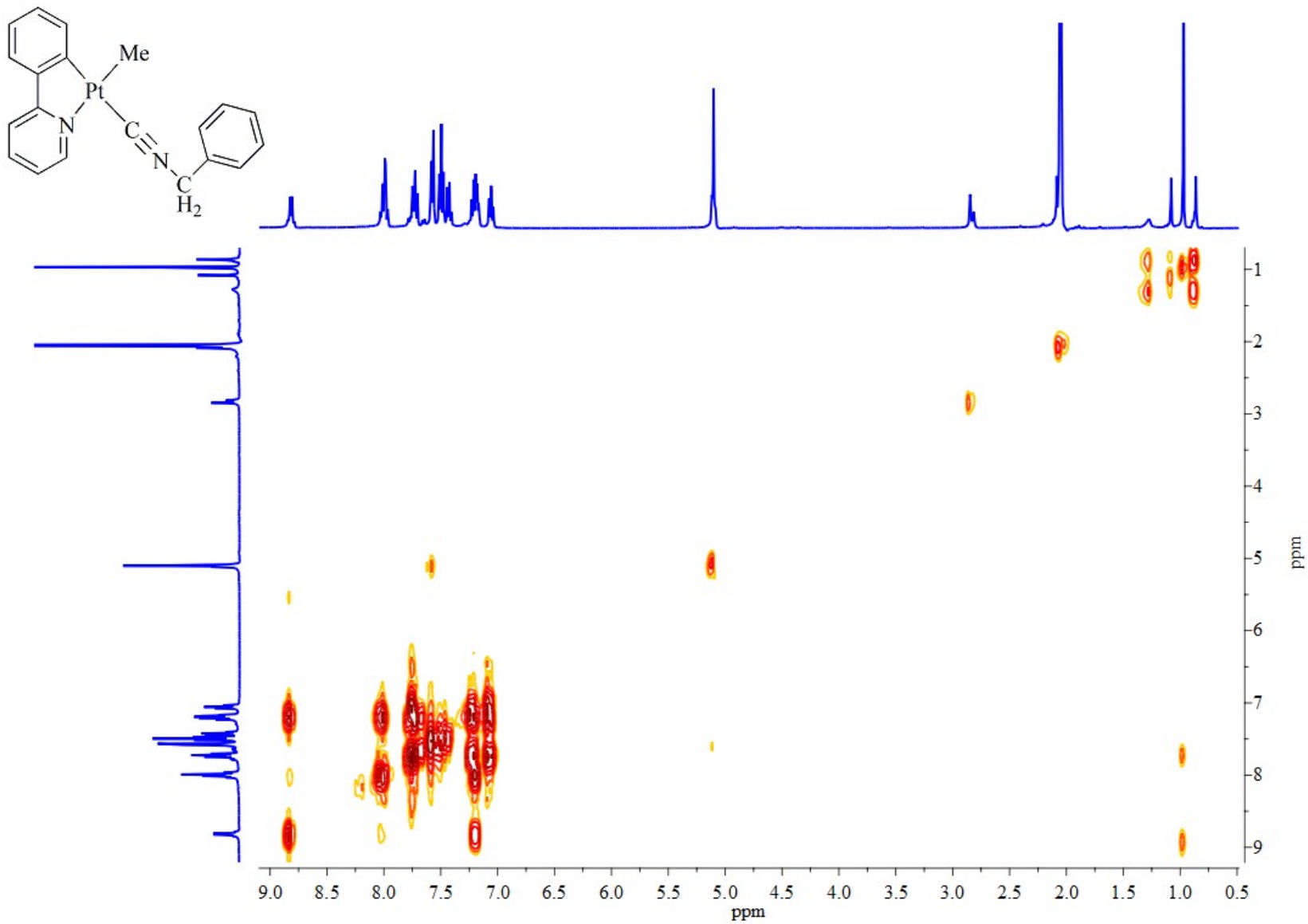

Figure S5. HHCOSY spectrum of [Pt(ppy)(Me)(CN-Bz)], **1**, in acetone d_6.

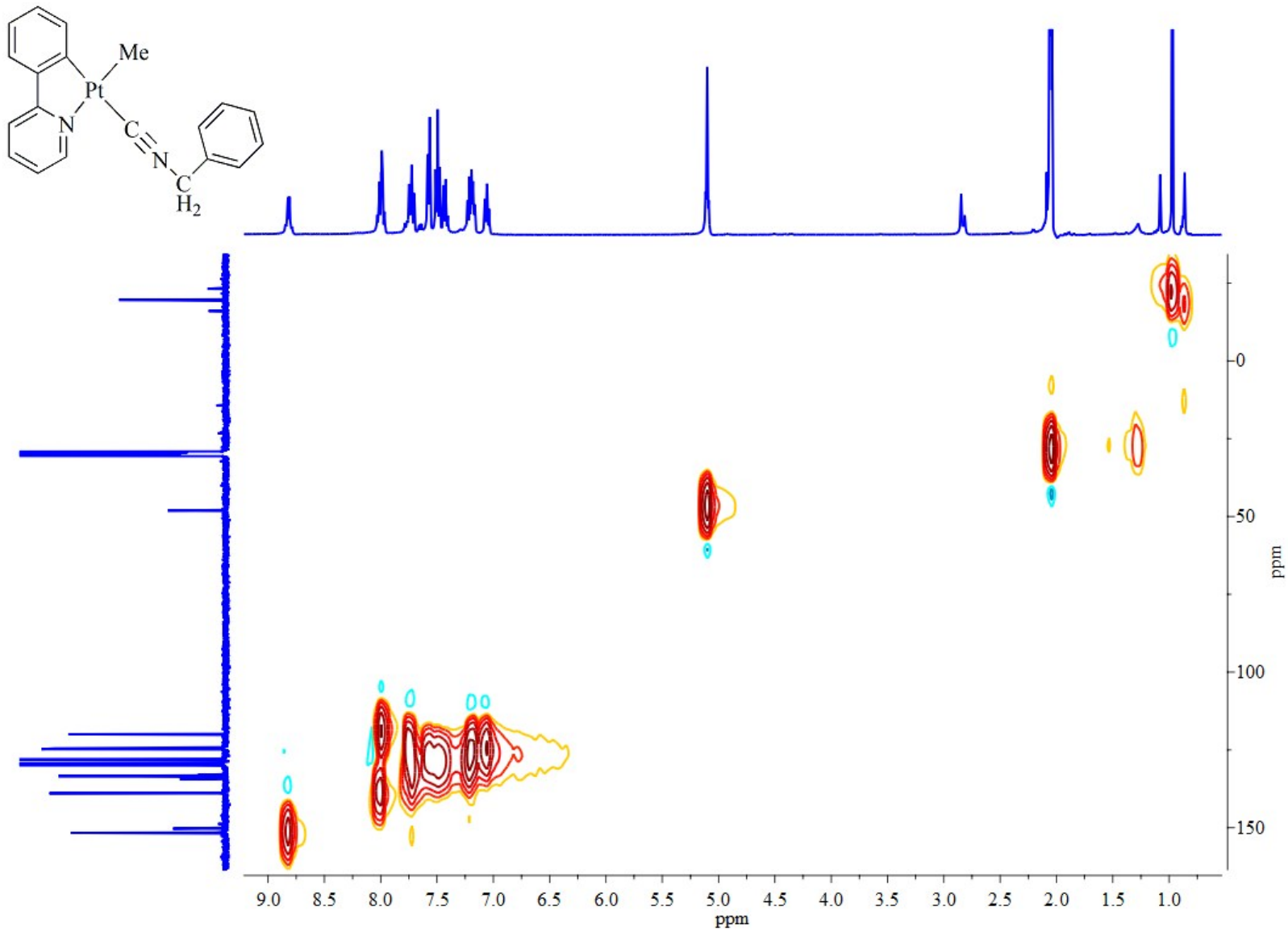

Figure S6. HSQC spectrum of [Pt(ppy)(Me)(CN-Bz)], **1**, in acetone d_6.

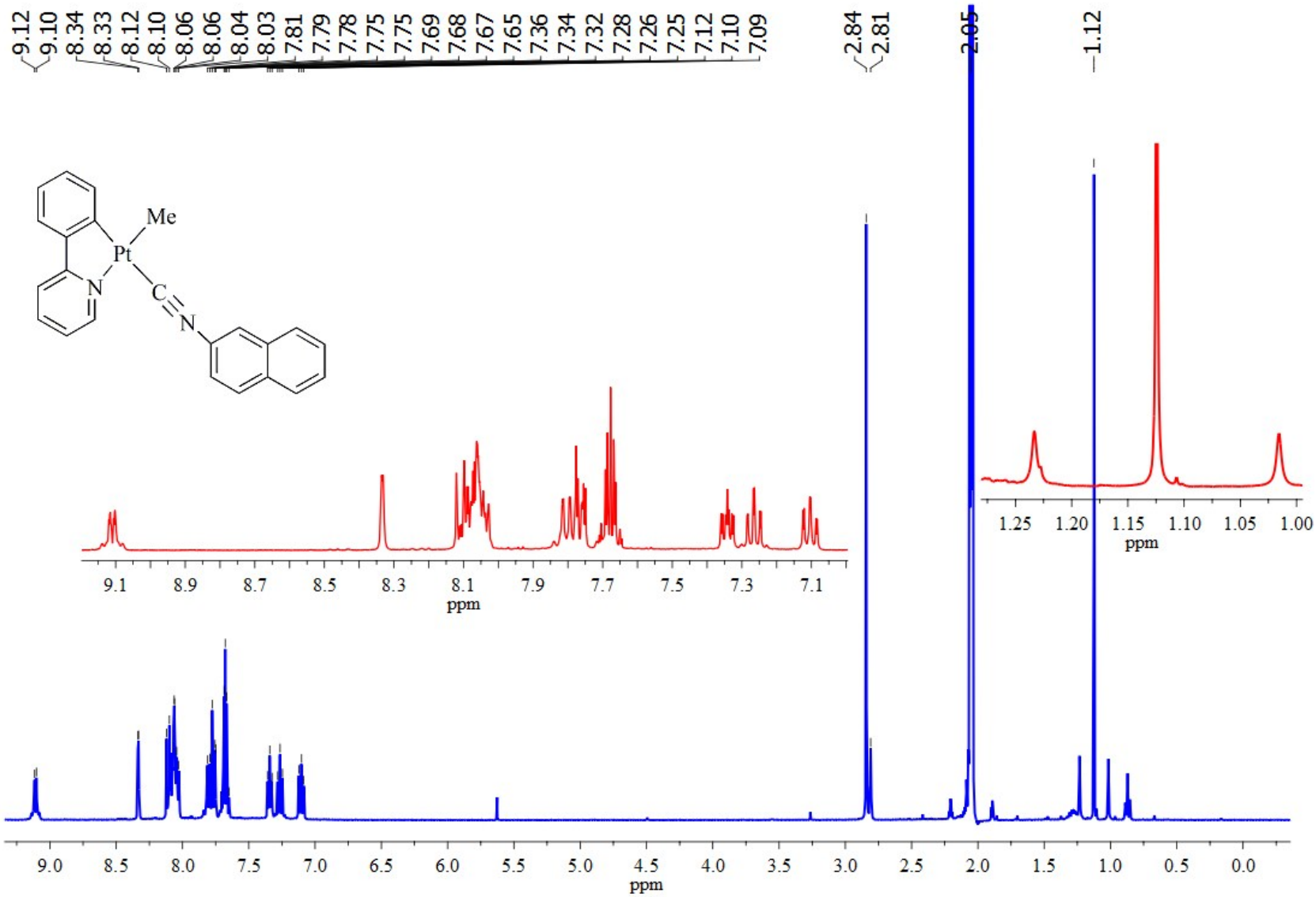

Figure S7. ^{1}HNMR spectrum of [Pt(ppy)(Me)(CN-2Np)], **2**, in acetone d_6.

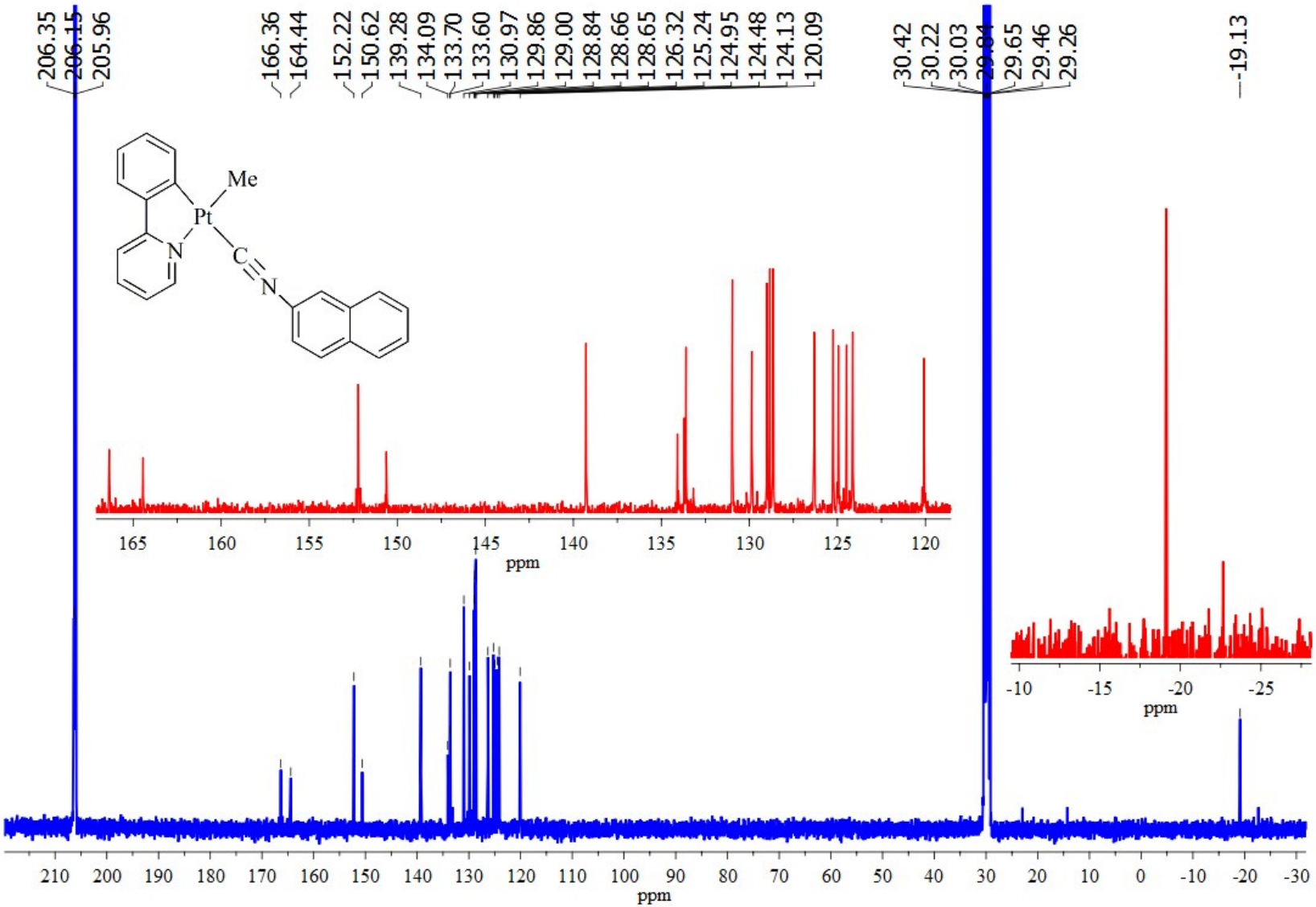

Figure S8. ^{13}CNMR spectrum of [Pt(ppy)(Me)(CN-2Np)], **2**, in acetone d_6.

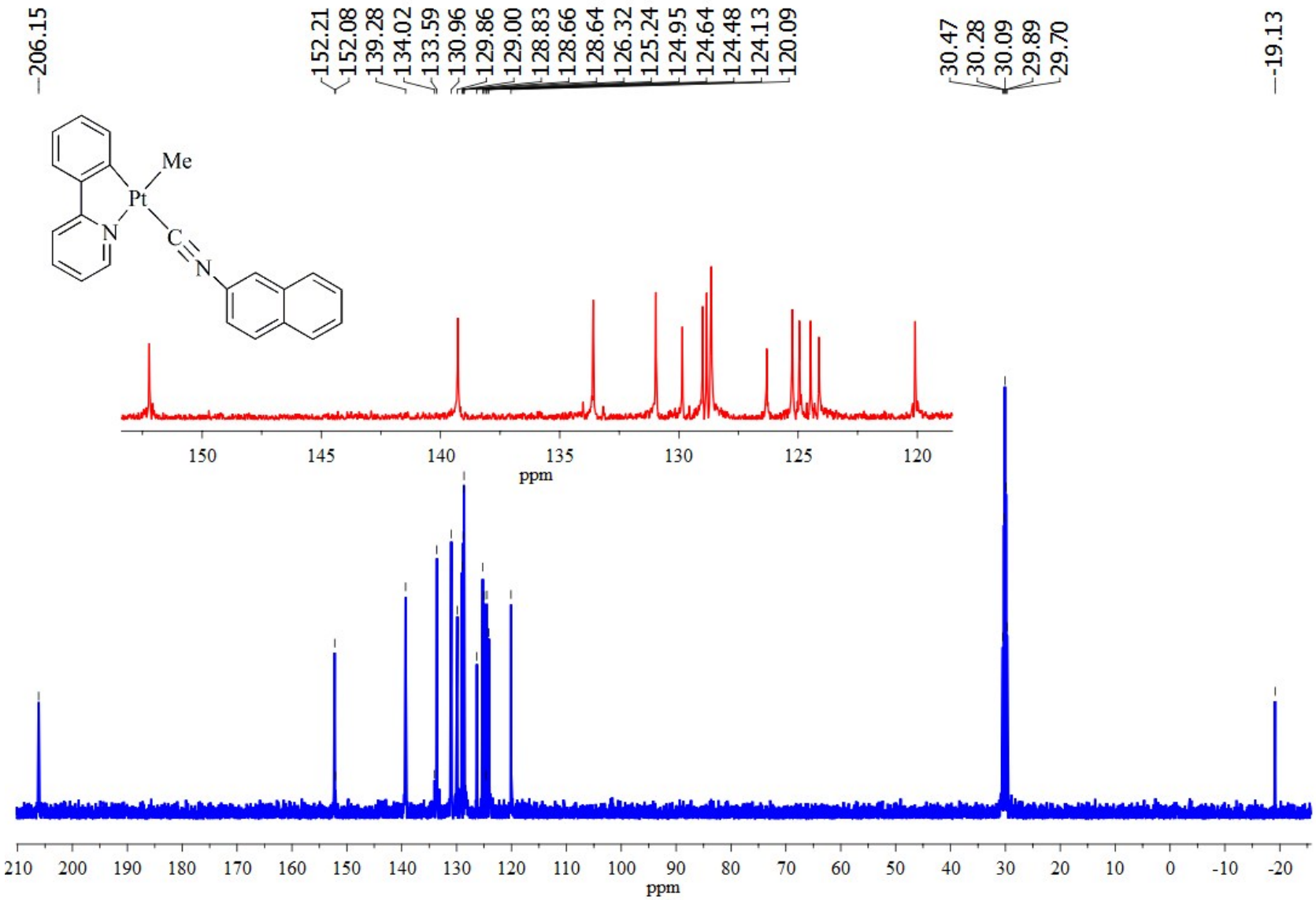

Figure S9. DEPT 135° spectrum of [Pt(ppy)(Me)(CN-2Np)], **2**, in acetone d_6.

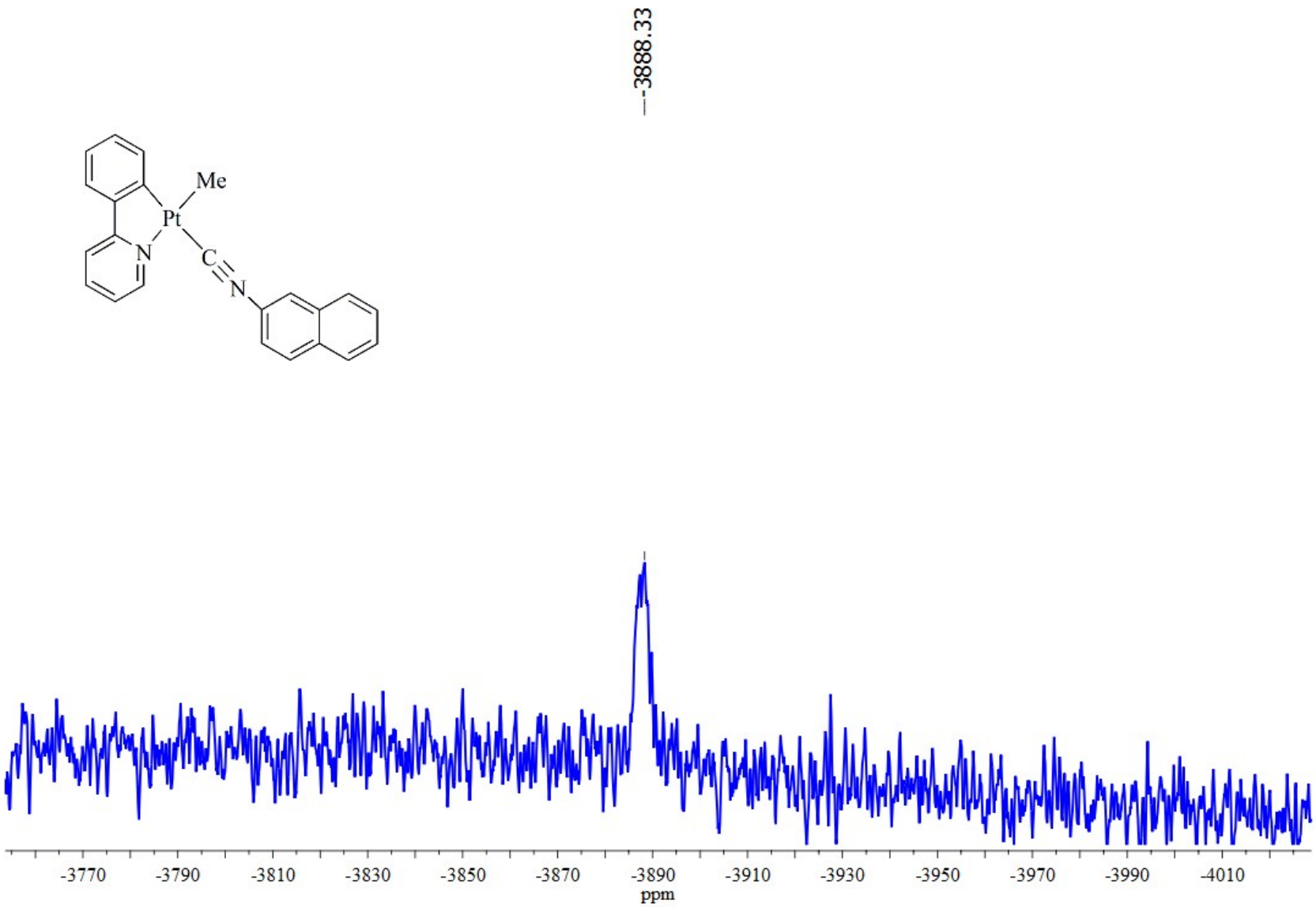

Figure S10. ^{195}PtNMR spectrum of [Pt(ppy)(Me)(CN-2Np)], **2**, in acetone d_6.

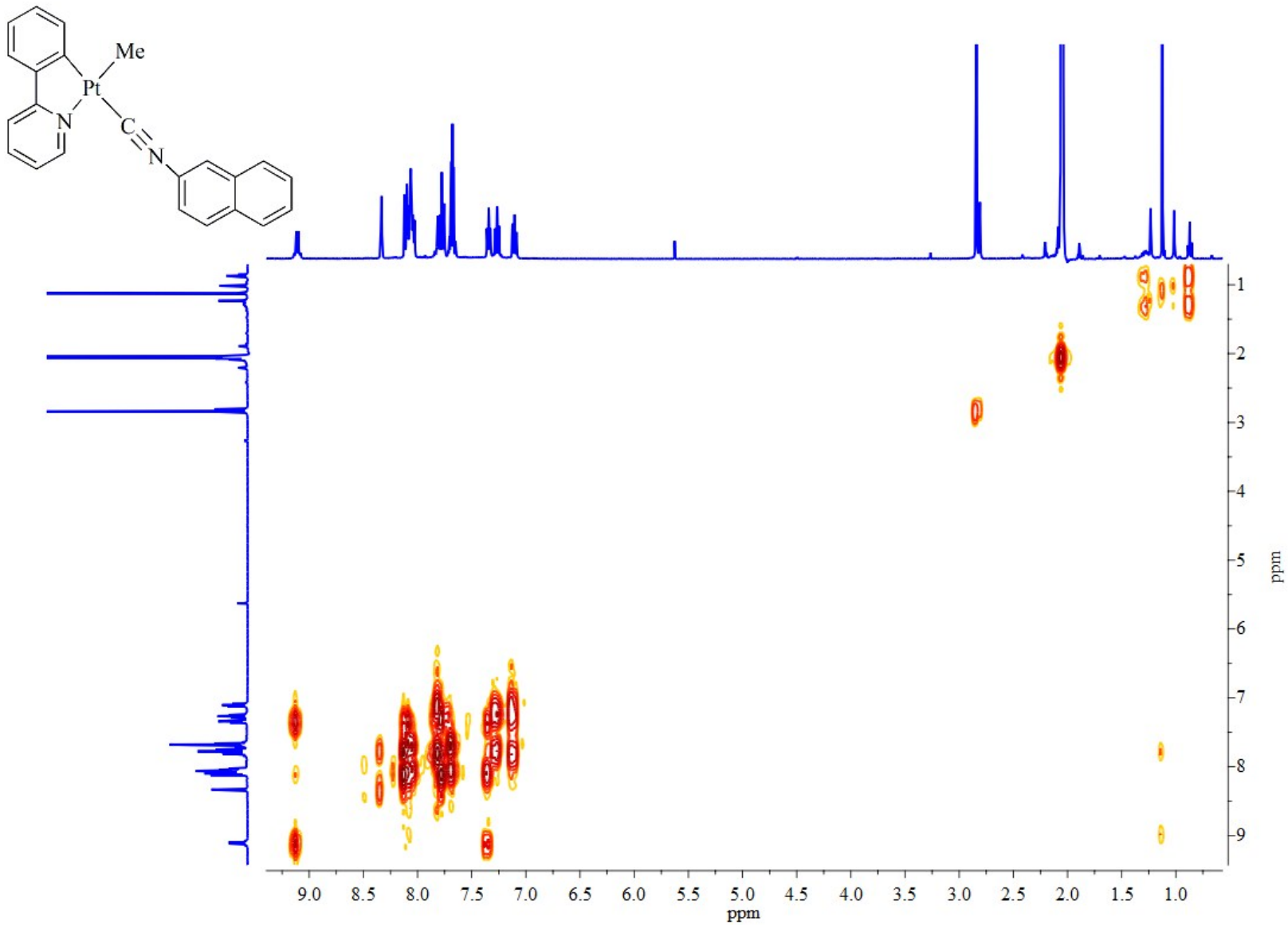

Figure S11. HHCOSY spectrum of [Pt(ppy)(Me)(CN-2Np)], **2**, in acetone d_6.

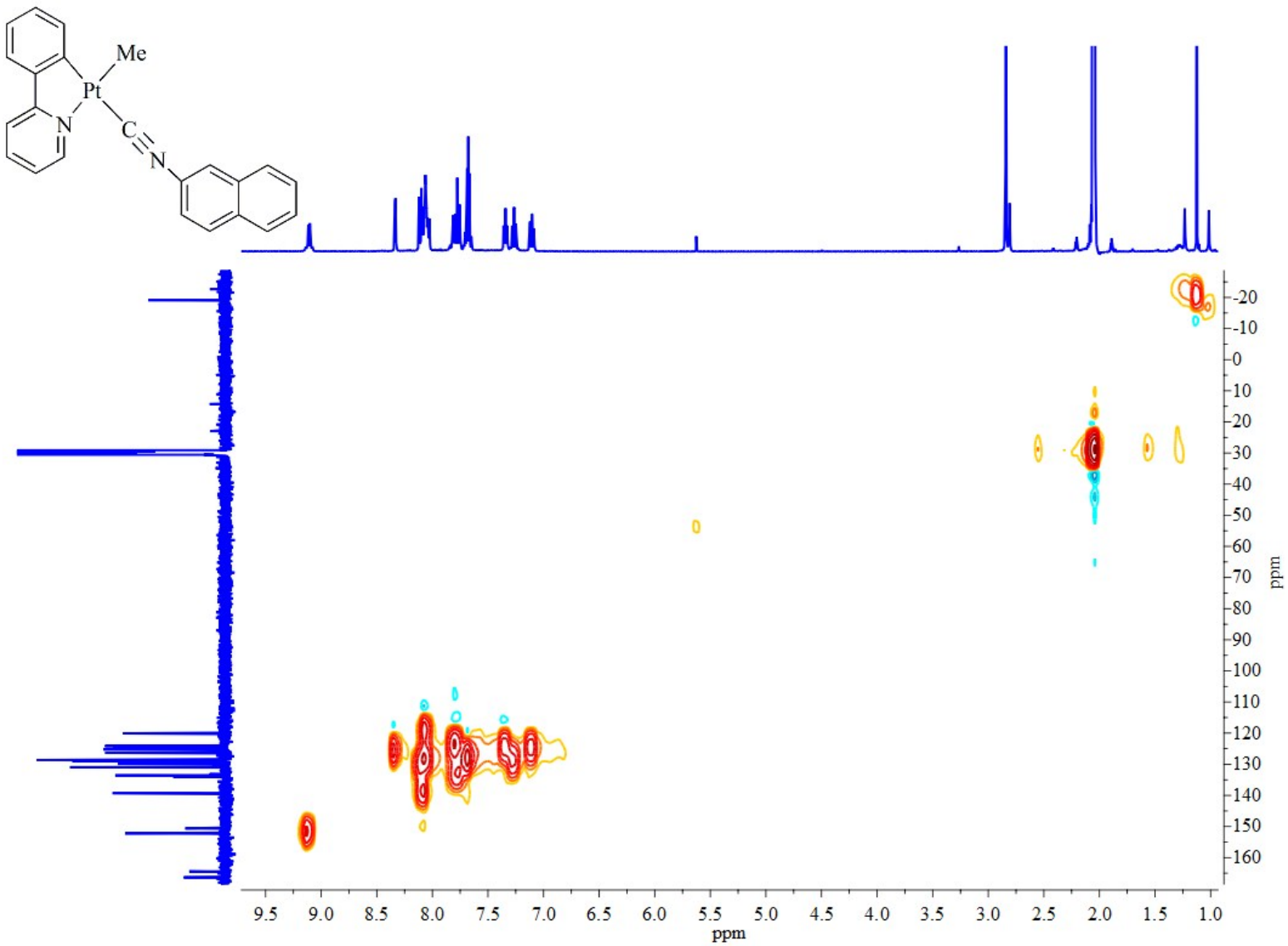

Figure S12. HSQC spectrum of [Pt(ppy)(Me)(CN-2Np)], **2**, in acetone d_6.

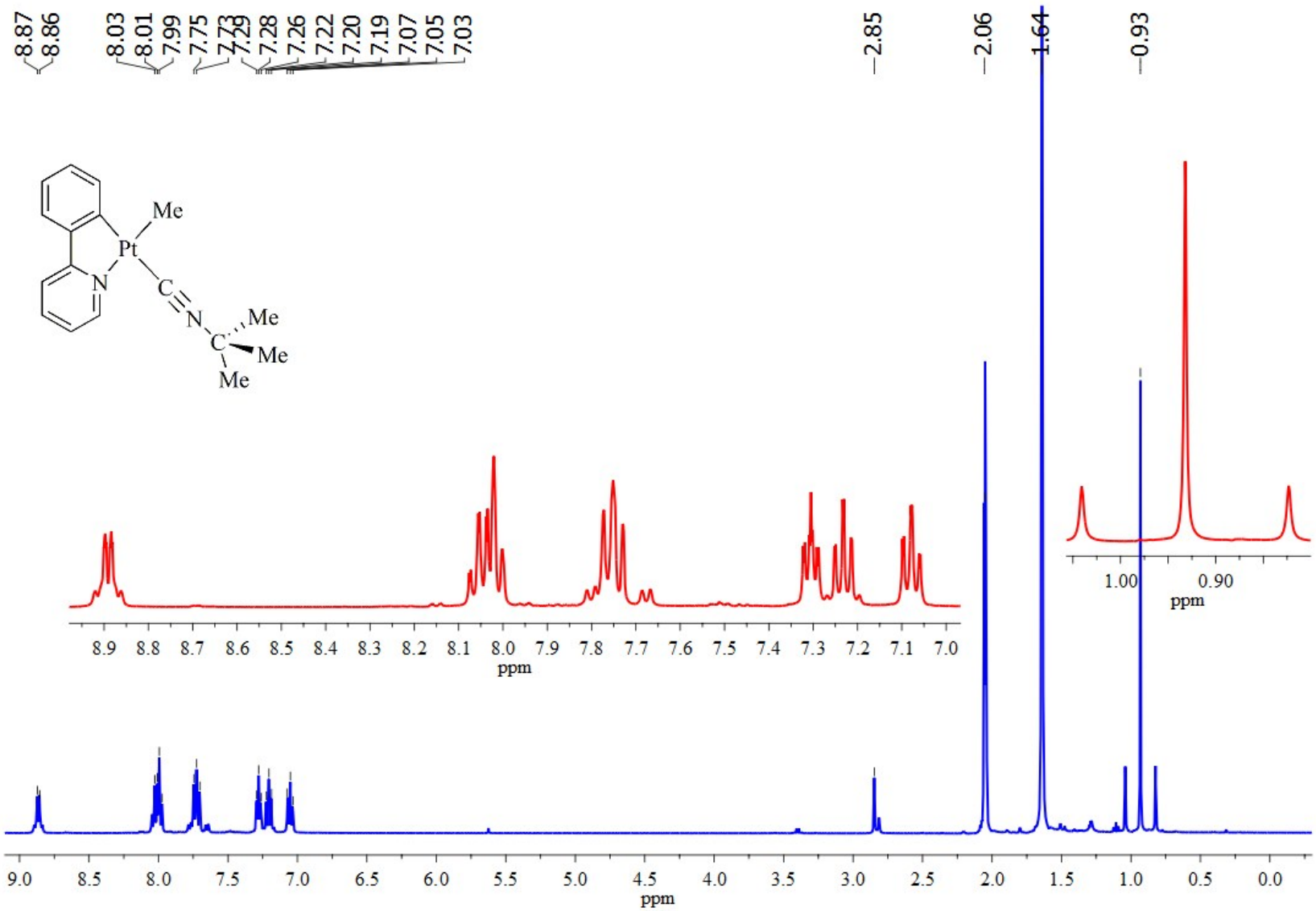

Figure S13. ^{1}HNMR spectrum of [Pt(ppy)(Me)(CN-tBu)], **3**, in acetone d_6.

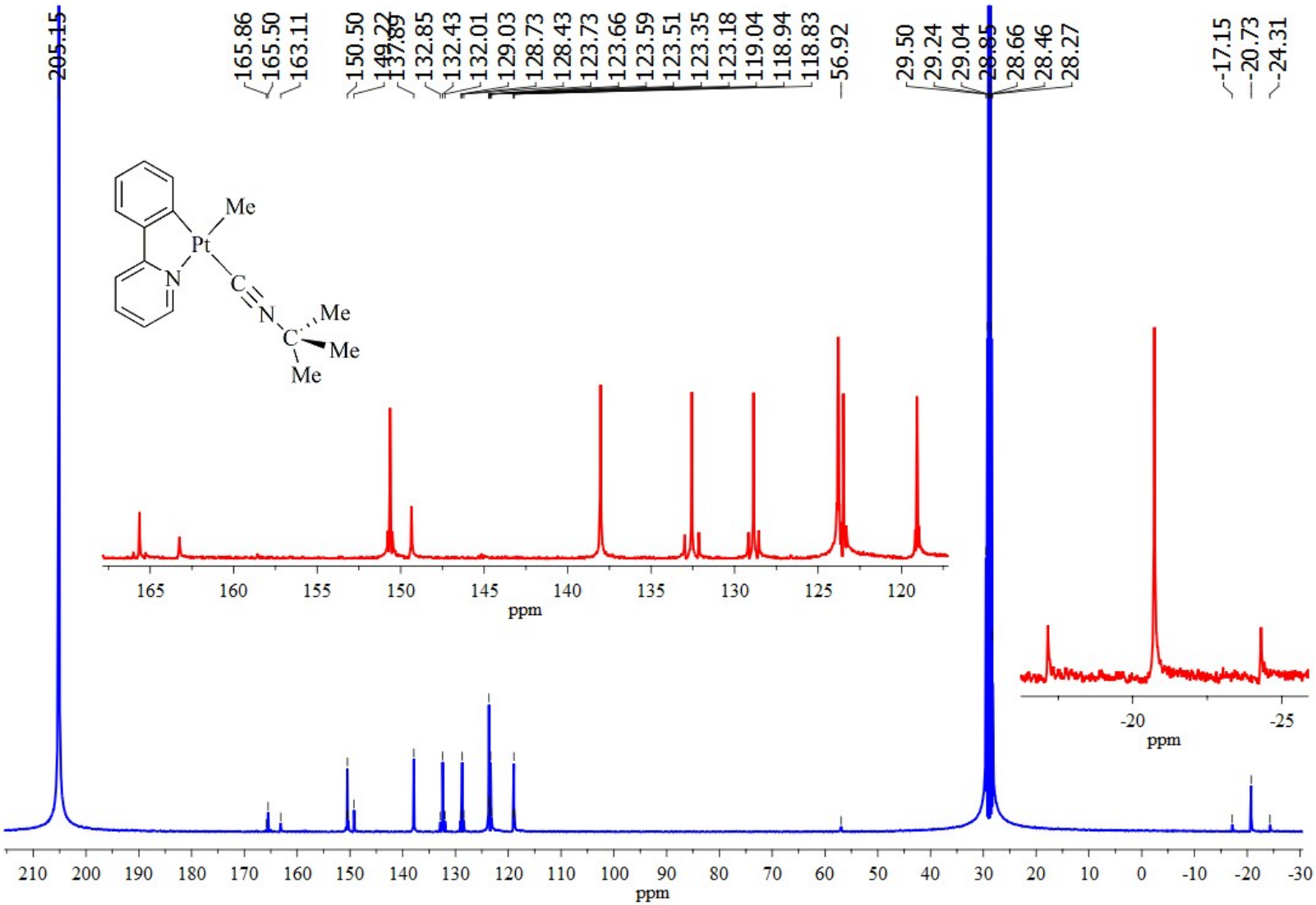

Figure S14. ^{13}CNMR spectrum of [Pt(ppy)(Me)(CN-tBu)], **3**, in acetone d_6.

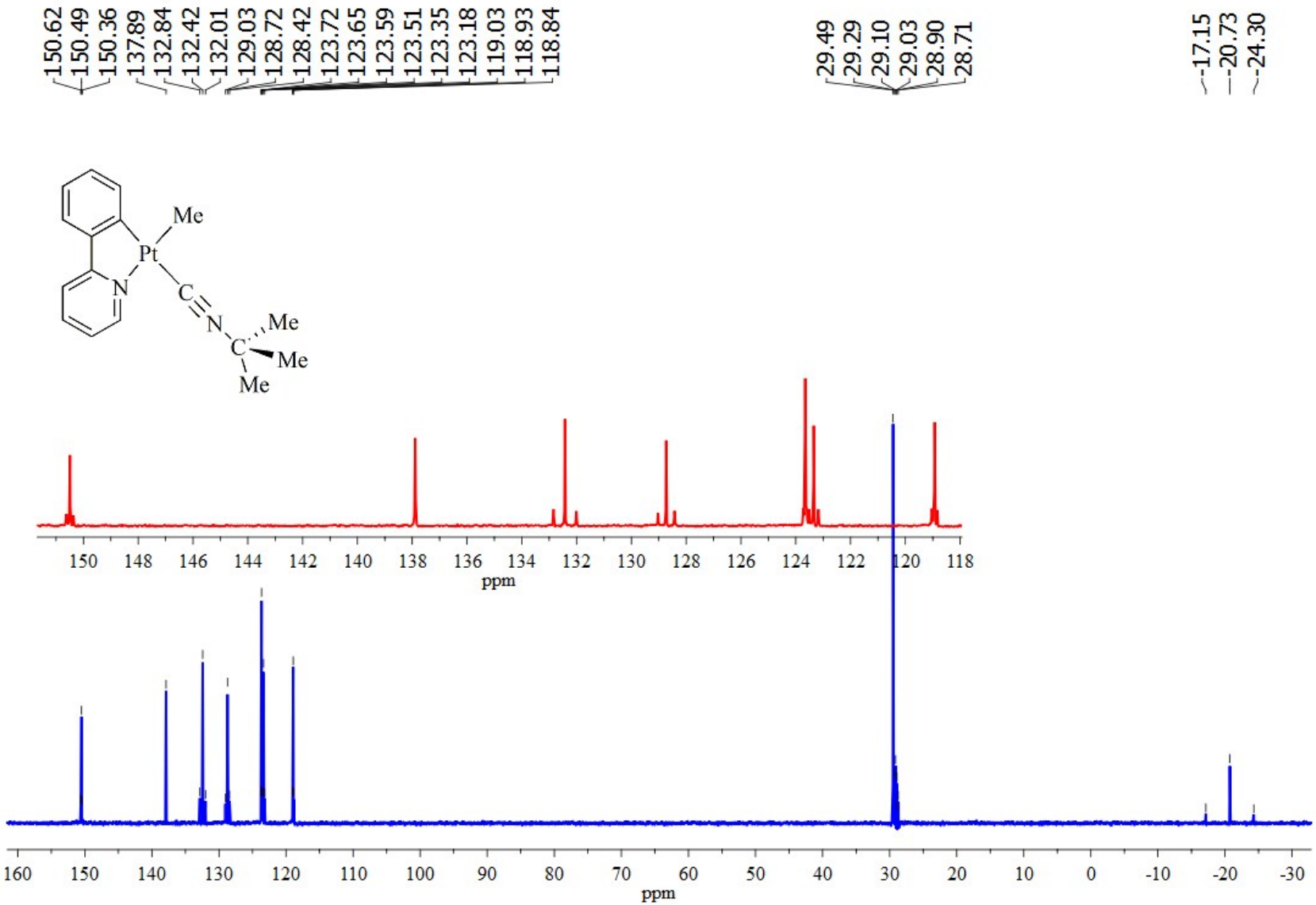

Figure S15. DEPT 135° spectrum of [Pt(ppy)(Me)(CN-tBu)], **3**, in acetone d_6.

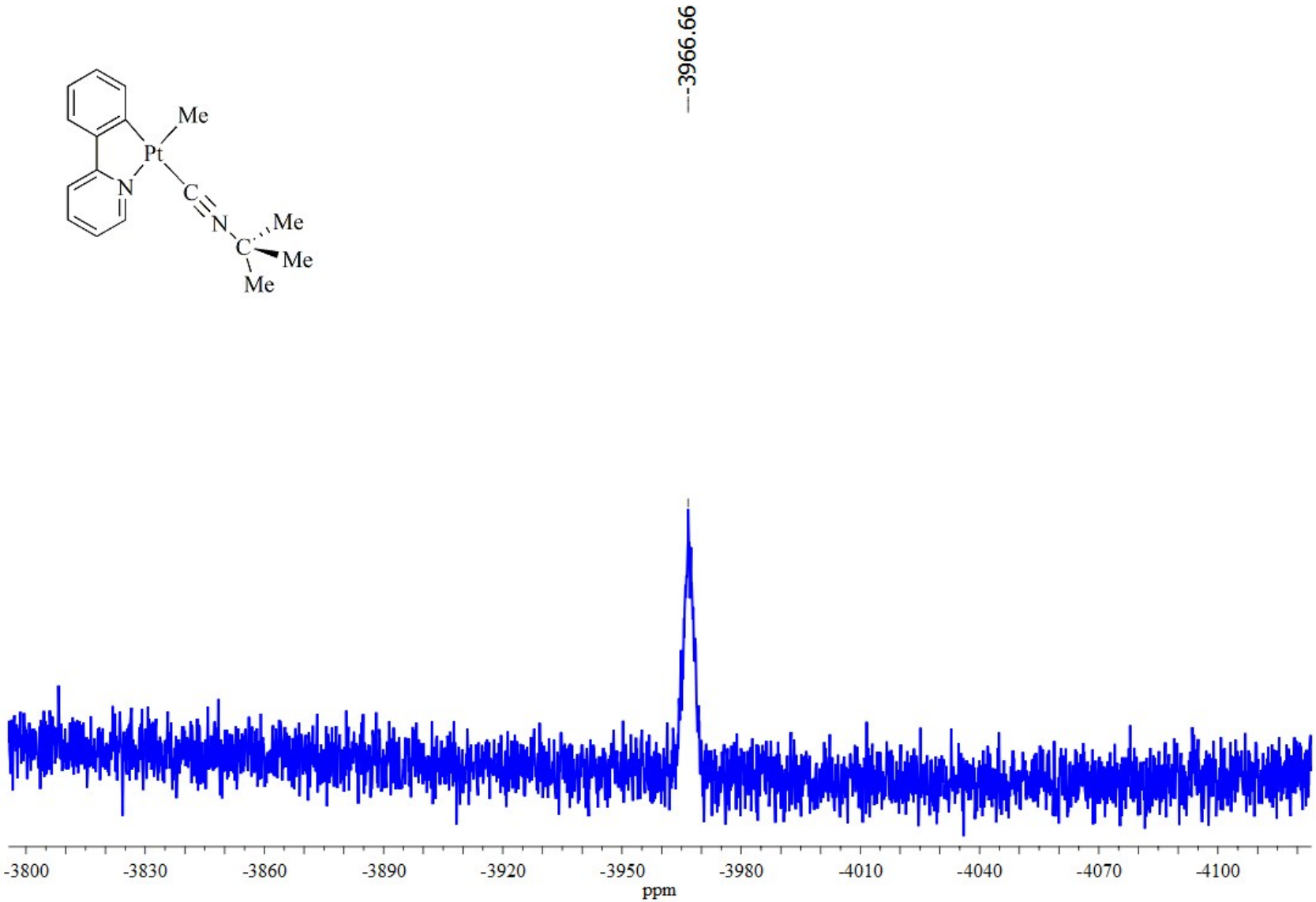

Figure S16. ^{195}PtNMR spectrum of [Pt(ppy)(Me)(CN-tBu)], **3**, in acetone d_6.

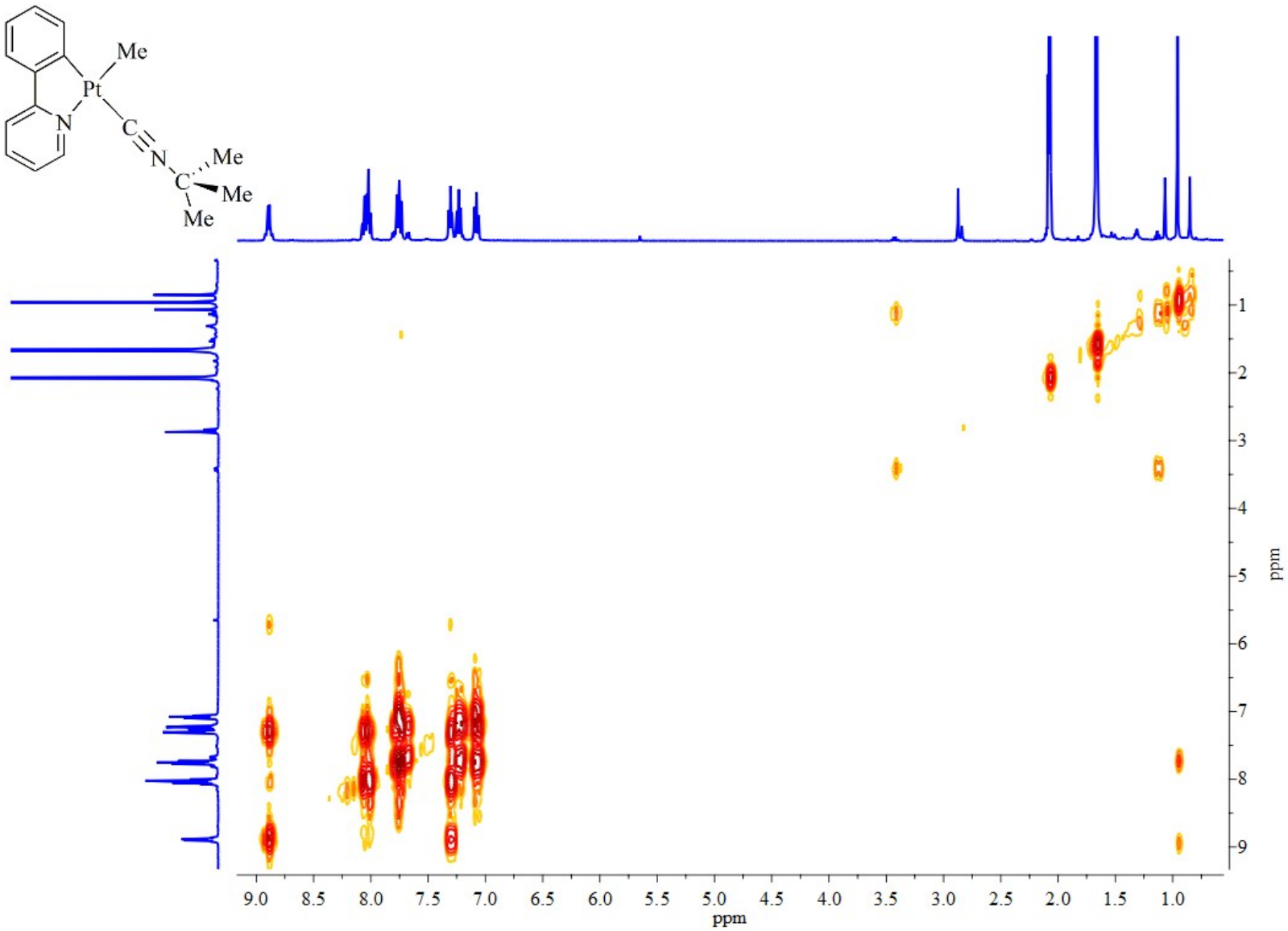

Figure S17. HHCOSY spectrum of [Pt(ppy)(Me)(CN-tBu)], **3**, in acetone d_6.

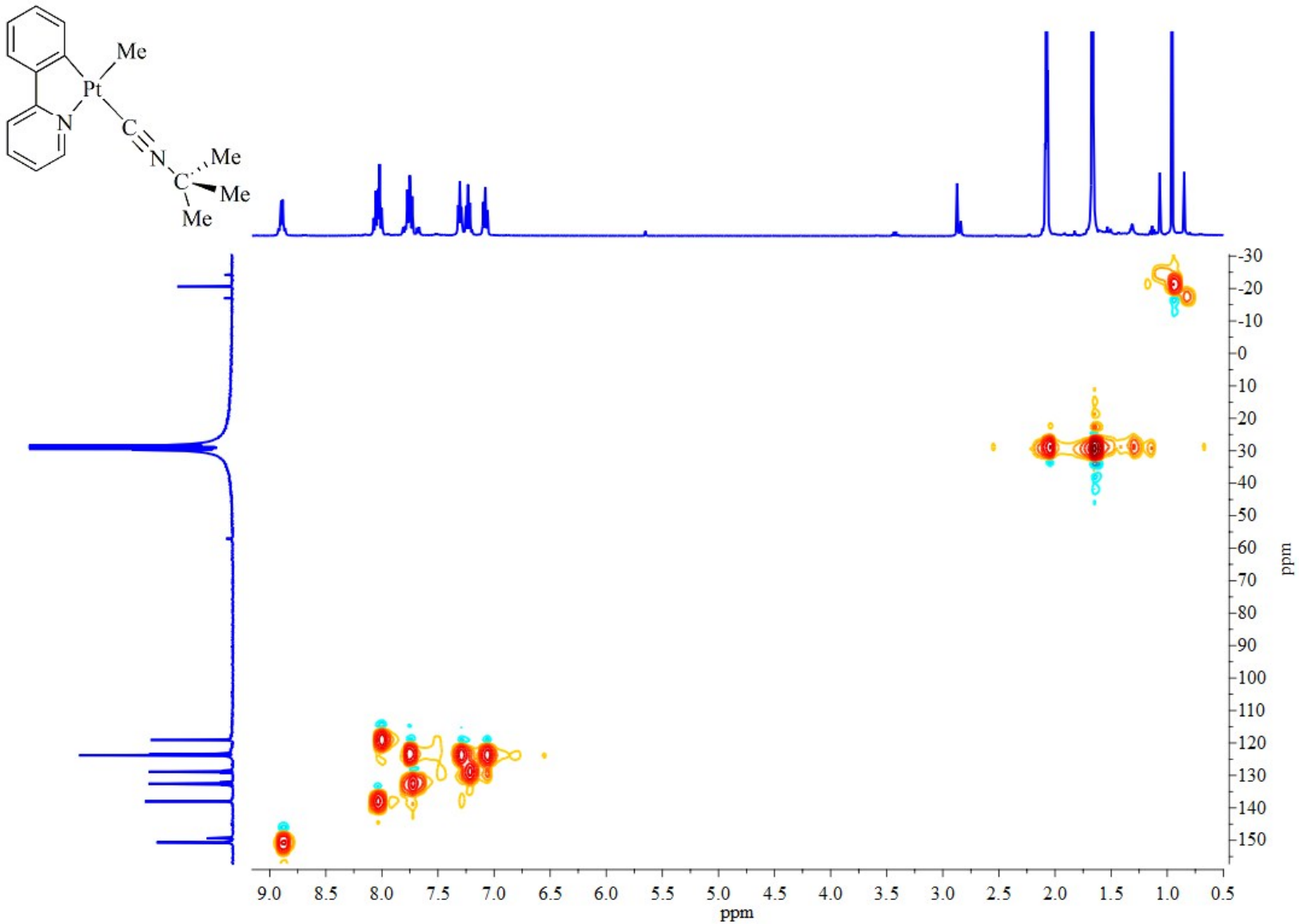

Figure S18. HSQC spectrum of [Pt(ppy)(Me)(CN-tBu)], **3**, in acetone d_6.

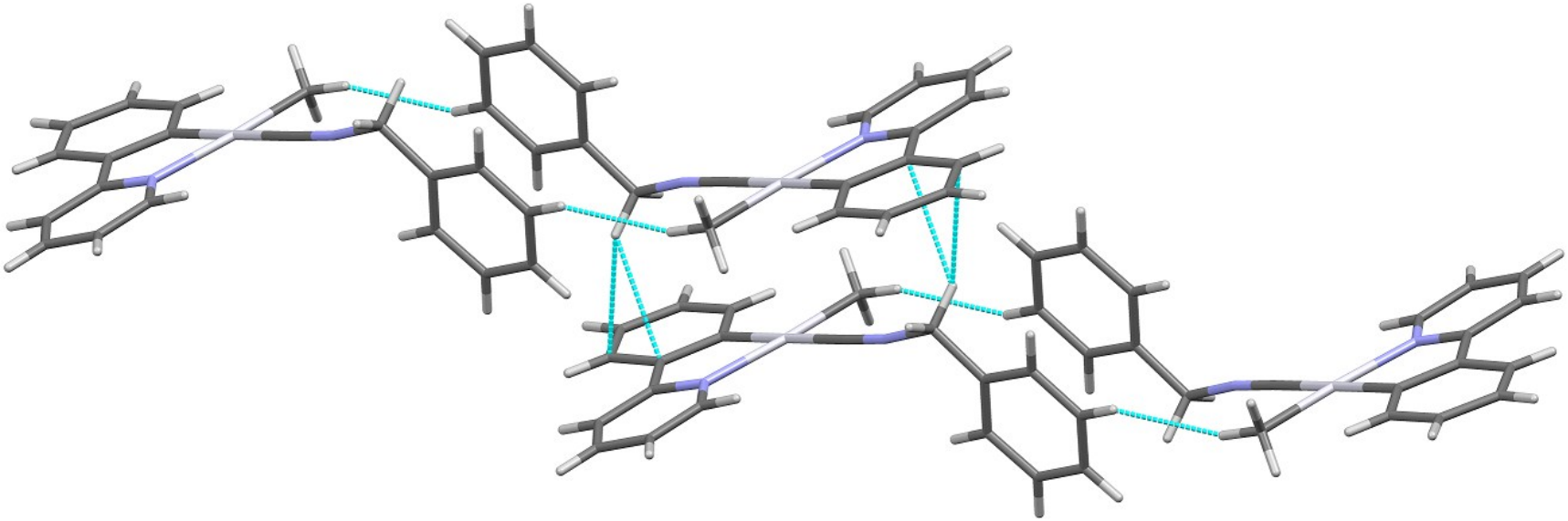

Figure S19. View of the crystal packing for the complex **1**.

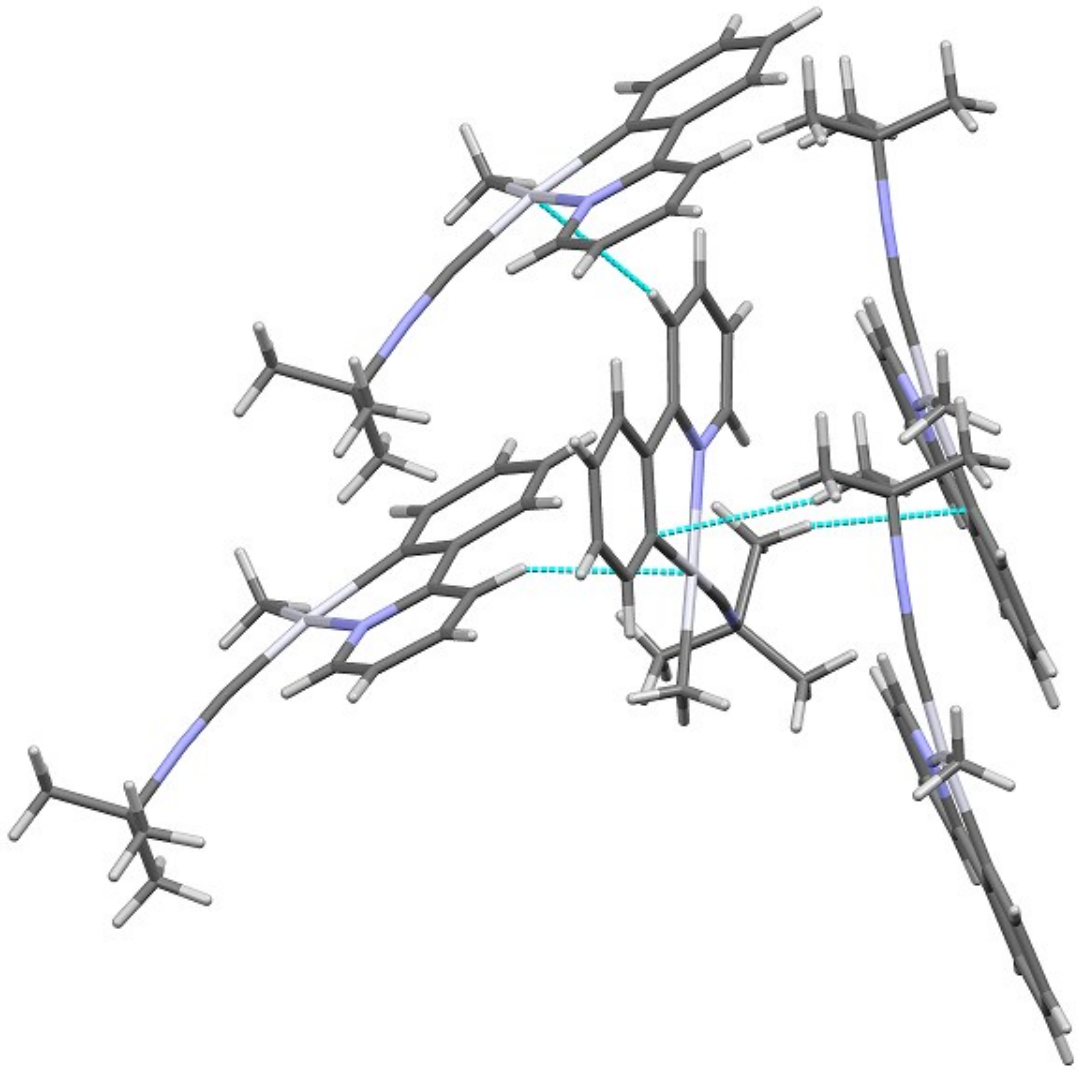

Figure S20. View of the crystal packing for the complex **3**.

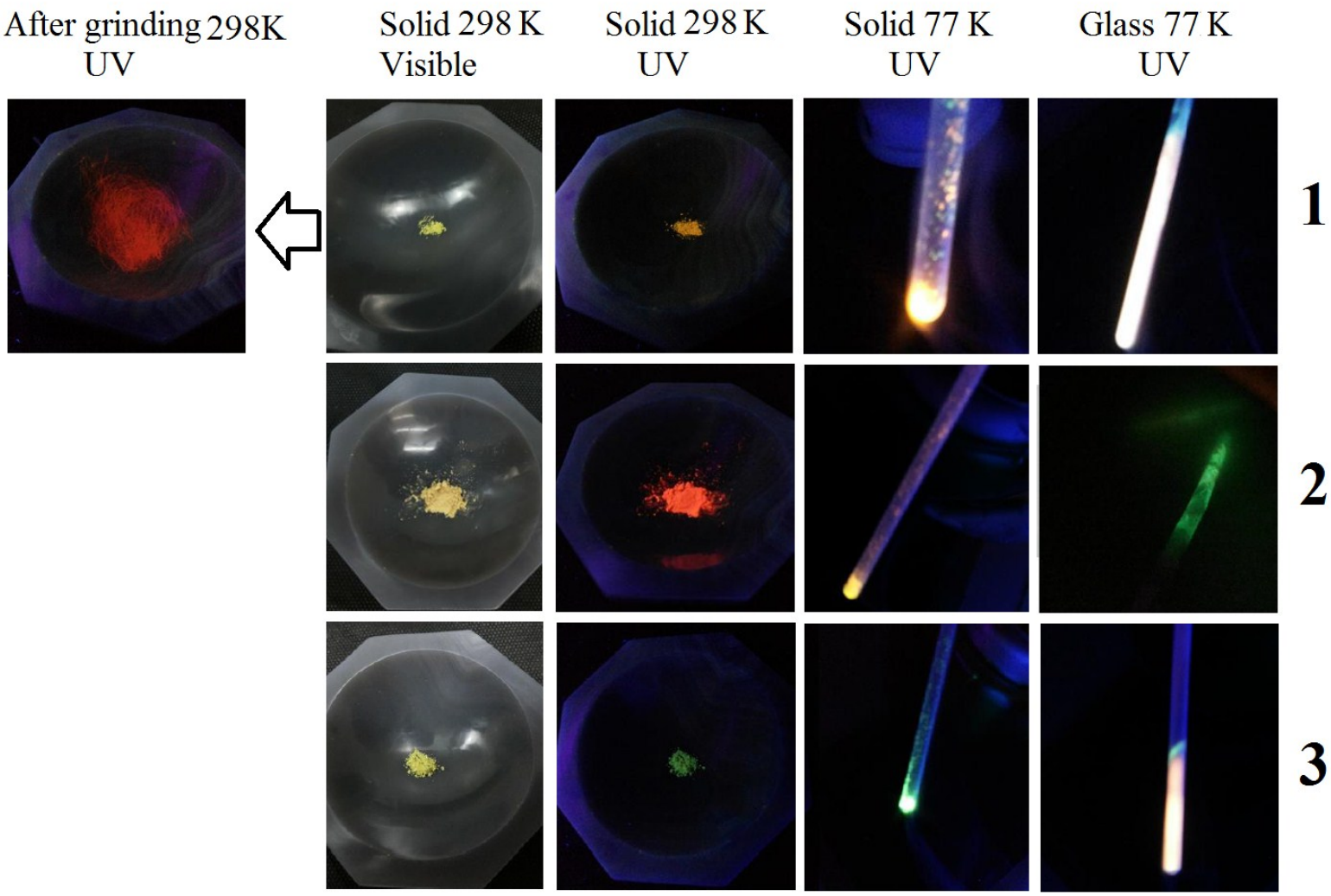

Figure S21. Photographic images of **1-3** under visible and UV light in the solid state at room (298 K) and low temperature (77 K) and CH_2Cl_2 glassy state (77 K).

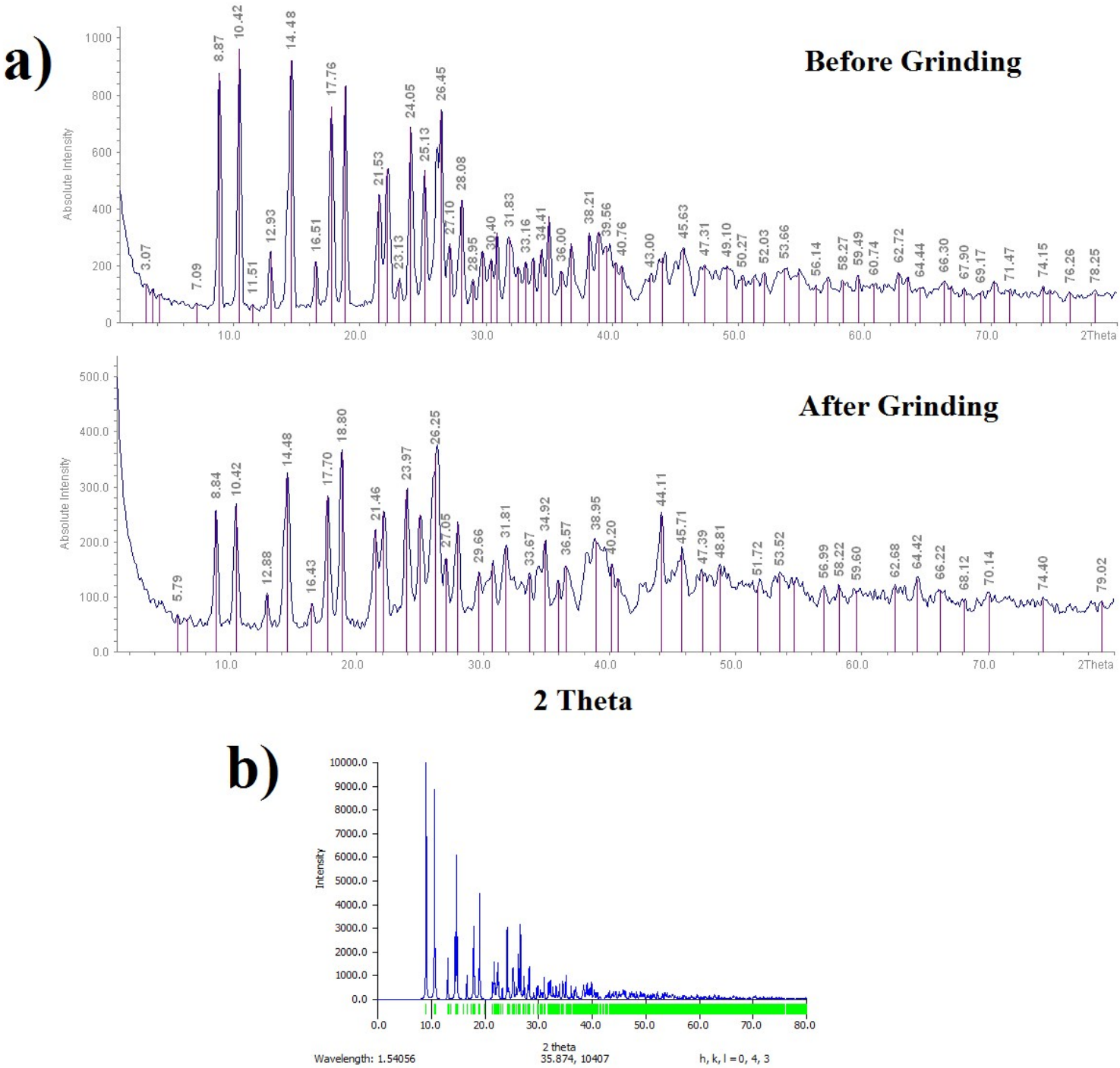

Figure S22. a) The XRD patterns for the complex **1** before and after grinding. b) Simulated PXRD pattern for the complex **1**.

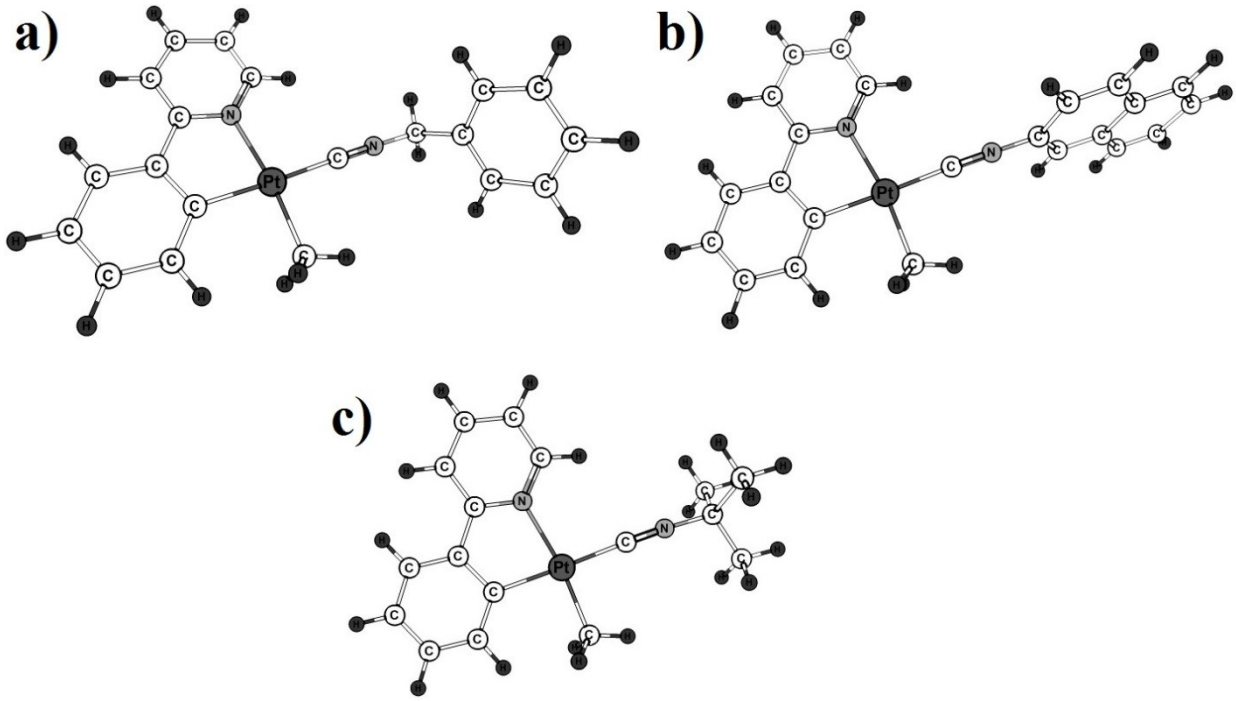

Figure S23. DFT optimized structures in ground state and gas phase for the complexes a) **1**, b) **2** and c) **3**.

Table S1. The energies of the selected MOs for the complex **1** and their compositions.

MO	Energy (eV)	Components (%)			
		Pt	ppy	CN-Bz	Me
LUMO+5	0.192	19	20	59	2
LUMO+4	-0.260	8	15	77	0
LUMO+3	-0.370	6	12	82	0
LUMO+2	-0.640	8	16	76	0
LUMO+1	-0.898	2	98	0	0
LUMO	-1.588	7	86	6	1
HOMO	-5.833	35	60	5	0
HOMO-1	-6.091	90	6	0	4
HOMO-2	-6.248	60	35	1	4
HOMO-3	-6.410	49	47	1	3
HOMO-4	-6.907	65	10	15	10
HOMO-5	-7.040	10	12	75	3

Table S2. The energies of the selected MOs for the complex **2** and their compositions.

MO	Energy (eV)	Components (%)			
		Pt	ppy	CN-2Np	Me
LUMO+5	-0.011	18	24	53	5
LUMO+4	-0.116	16	34	47	3
LUMO+3	-0.918	2	98	0	0
LUMO+2	-0.996	3	12	85	0
LUMO+1	-1.453	3	58	39	0
LUMO	-1.860	7	29	63	1
HOMO	-5.805	33	48	19	0
HOMO-1	-6.166	80	8	0	2
HOMO-2	-6.221	14	37	47	2
HOMO-3	-6.345	40	28	29	3
HOMO-4	-6.469	58	34	4	4
HOMO-5	-6.903	7	16	77	0

Table S3. The energies of the selected MOs for the complex **3** and their compositions.

MO	Energy (eV)	Components (%)			
		Pt	ppy	CN-tBu	Me
LUMO+5	0.832	49	12	21	18
LUMO+4	0.697	19	69	11	1
LUMO+3	0.184	20	22	50	8
LUMO+2	-0.407	20	43	37	0
LUMO+1	-0.892	2	98	0	0
LUMO	-1.572	7	88	5	0
HOMO	-5.814	36	59	5	0
HOMO-1	-6.069	90	6	0	4
HOMO-2	-6.229	63	32	1	4
HOMO-3	-6.396	46	51	1	2
HOMO-4	-6.890	70	11	15	4
HOMO-5	-7.145	23	45	7	25

Table S4. The MO plots for the complex **1**.

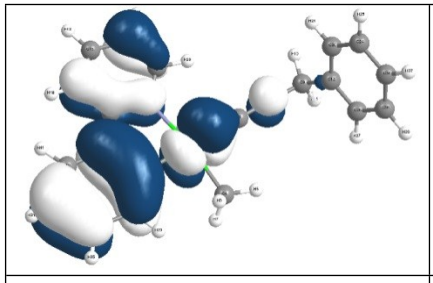	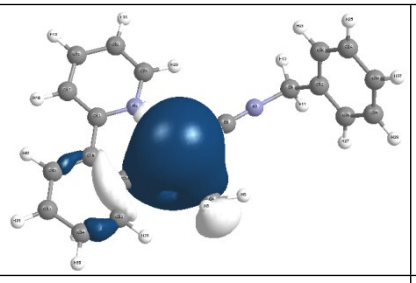	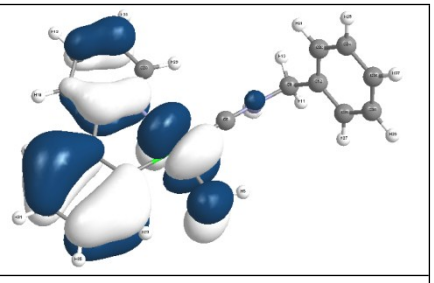
HOMO	HOMO-1	HOMO-2
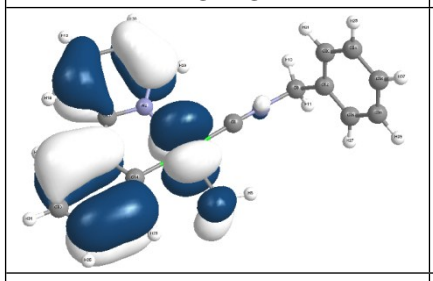	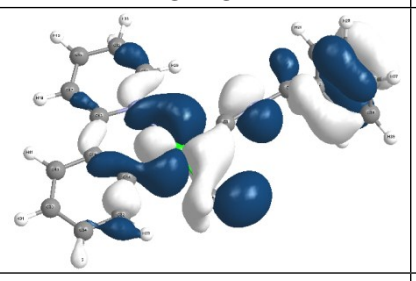	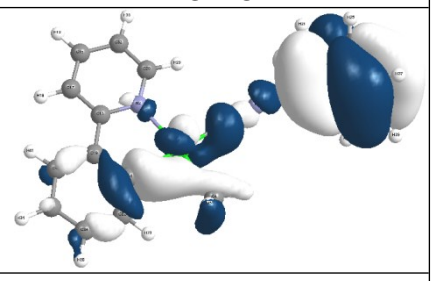
HOMO-3	HOMO-4	HOMO-5
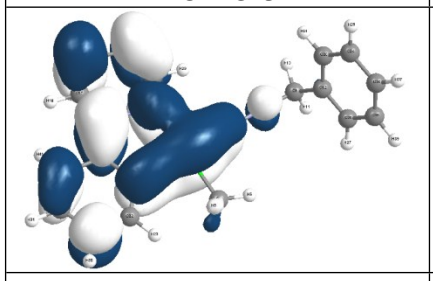	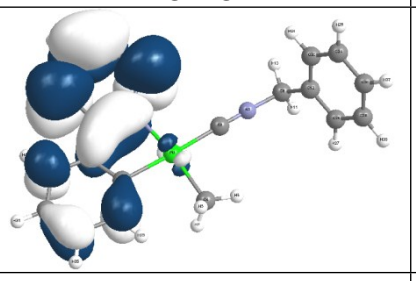	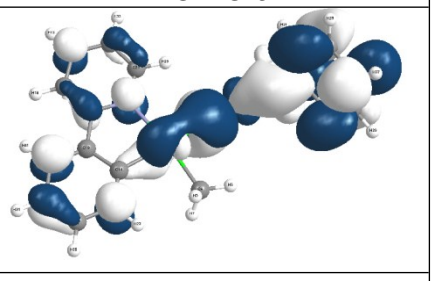
LUMO	LUMO+1	LUMO+2
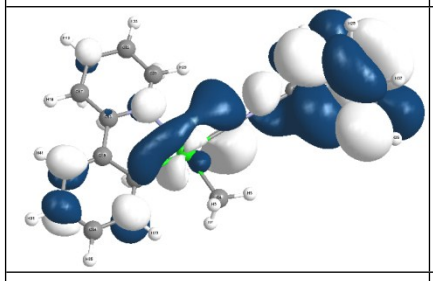	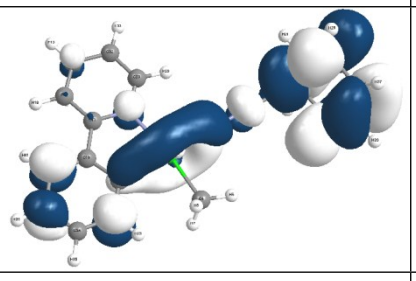	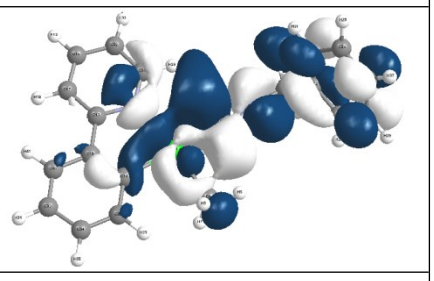
LUMO+3	LUMO+4	LUMO+5

Table S5. The MO plots for the complex **2**.

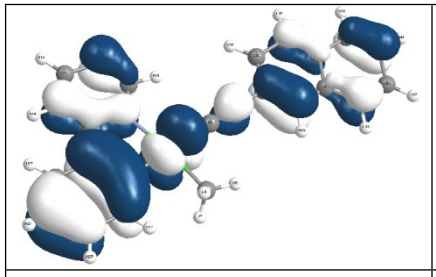	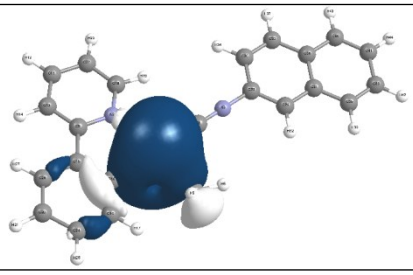	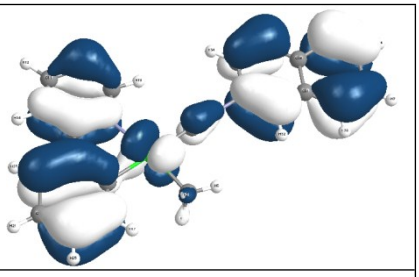
HOMO	HOMO-1	HOMO-2
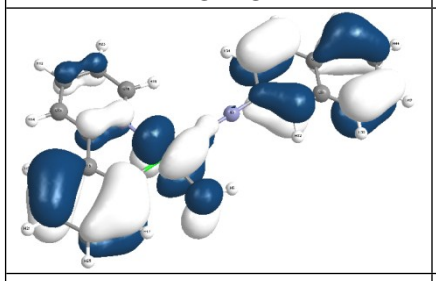	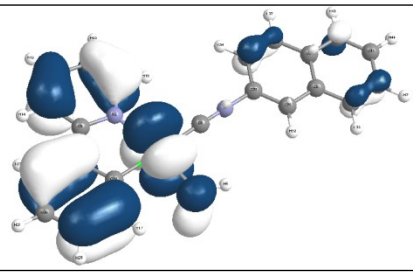	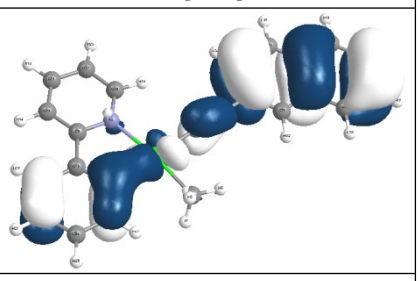
HOMO-3	HOMO-4	HOMO-5
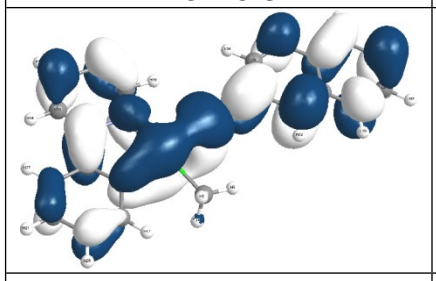	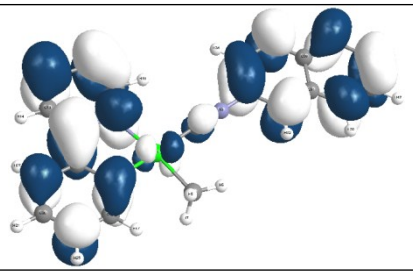	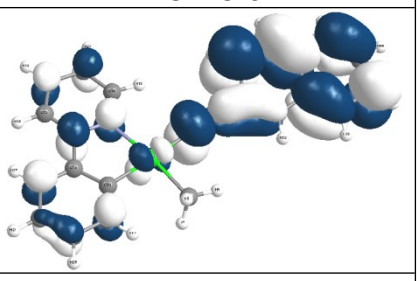
LUMO	LUMO+1	LUMO+2
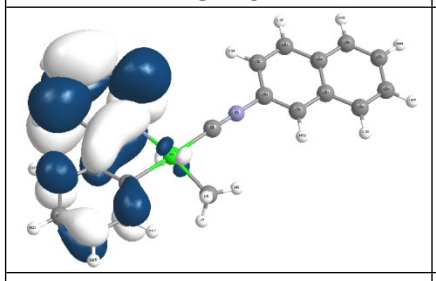	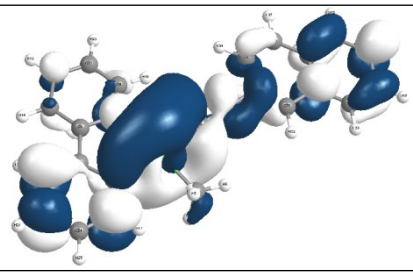	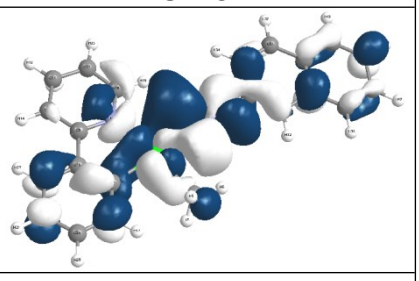
LUMO+3	LUMO+4	LUMO+5

Table S6. The MO plots for the complex **3**.

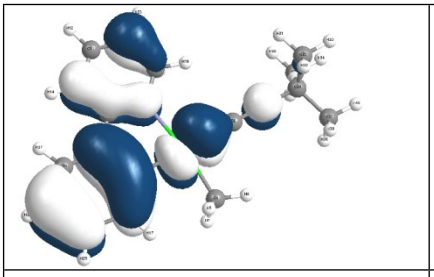	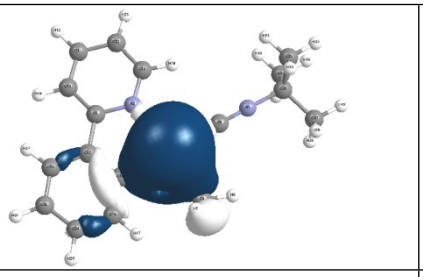	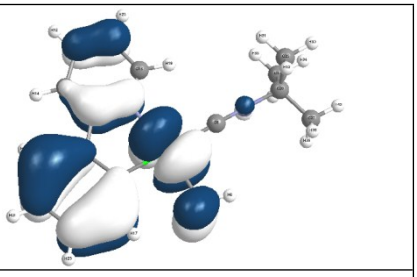
HOMO	HOMO-1	HOMO-2
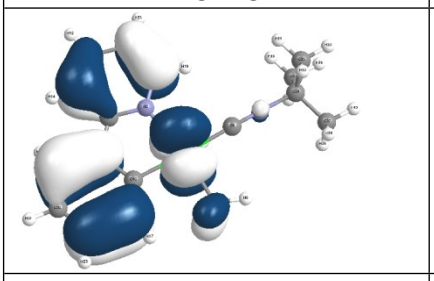	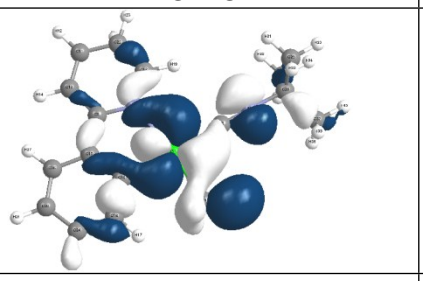	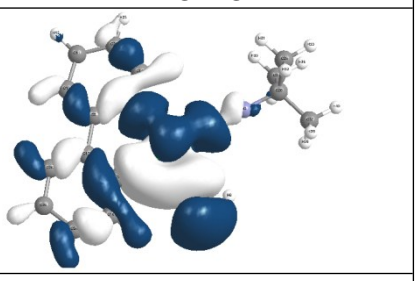
HOMO-3	HOMO-4	HOMO-5
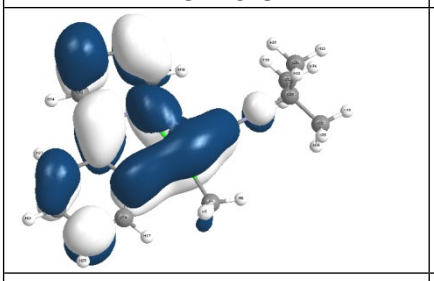	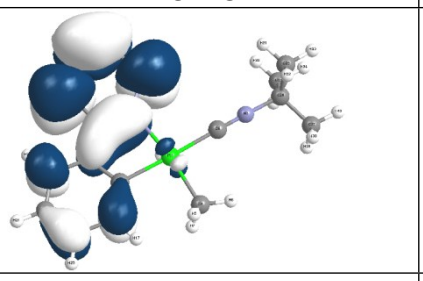	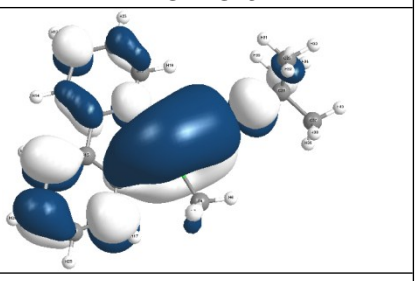
LUMO	LUMO+1	LUMO+2
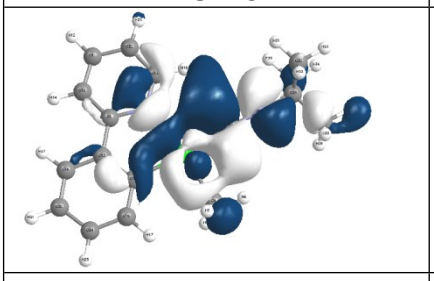	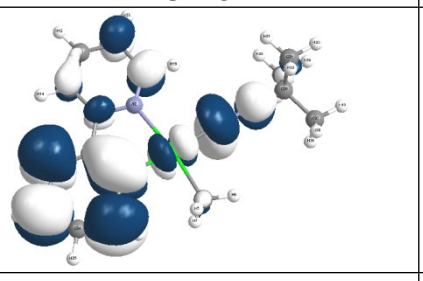	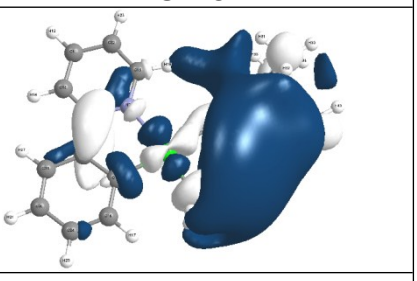
LUMO+3	LUMO+4	LUMO+5

Table S7. Wavelengths and corresponding nature of transitions for the complex **1** where M = Pt, L = ppy and L′ = CN-Bz.

Excited state	Oscillator strength	Calculated λ (nm)	Transitions (Major Contribution)	Assignment
$S_0 \rightarrow S_1$	0.0494	353	HOMO→LUMO (95%)	ILCT, MLCT
$S_0 \rightarrow S_3$	0.1198	317	H-3→LUMO (13%)	ILCT, MLCT
			H-2→LUMO (80%)	MLCT, ILCT
$S_0 \rightarrow S_4$	0.0507	302	H-3→LUMO (49%)	ILCT, MLCT
			H-2→LUMO (11%)	MLCT, ILCT
			HOMO→L+1 (34%)	ILCT, MLCT, L′LCT
$S_0 \rightarrow S_5$	0.2094	283	H-3→LUMO (25%)	ILCT, MLCT
			HOMO→L+1 (61%)	ILCT, MLCT, L′LCT
$S_0 \rightarrow S_8$	0.1635	270	H-2→L+1 (32%)	MLCT, ILCT
			H-1→L+2 (11%)	ML′CT, MLCT
			HOMO→L+2 (38%)	ML′CT, LL′CT, ILCT
$S_0 \rightarrow S_{11}$	0.1786	264	H-2→L+1 (40%)	MLCT, ILCT
			HOMO→L+2 (21%)	ML′CT, LL′CT, ILCT
$S_0 \rightarrow S_{13}$	0.1770	256	HOMO→L+3 (42%)	ML′CT, LL′CT, ILCT
			HOMO→L+5 (13%)	ML′CT, LL′CT, ILCT

Table S8. Wavelengths and corresponding nature of transitions for the complex **2** where M = Pt, L = ppy and L′ = CN-2Np.

Excited state	Oscillator strength	Calculated λ (nm)	Transitions (Major Contribution)	Assignment
$S_0 \rightarrow S_1$	0.2852	369	HOMO→LUMO (87%)	ML′CT, LL′CT, ILCT
$S_0 \rightarrow S_3$	0.1958	333	H-4→LUMO (22%)	ML′CT, LL′CT, ILCT
			H-3→LUMO (37%)	ML′CT, ILCT, IL′CT
			H-2→LUMO (34%)	IL′CT, ILCT, ML′CT, LL′CT
$S_0 \rightarrow S_4$	0.1314	324	HOMO→L+1 (77%)	IL′CT, ILCT, ML′CT, MLCT
$S_0 \rightarrow S_5$	0.1430	314	H-3→LUMO (32%)	ML′CT, ILCT, IL′CT
			H-2→LUMO (45%)	IL′CT, ILCT, ML′CT, LL′CT
$S_0 \rightarrow S_7$	0.1196	309	H-4→LUMO (51%)	ML′CT, LL′CT, ILCT
			H-3→LUMO (14%)	ML′CT, ILCT, IL′CT
			HOMO→L+3 (10%)	MLCT, ILCT
$S_0 \rightarrow S_{12}$	0.1941	281	H-4→L+1 (13%)	MLCT, ML′CT
			H-3→L+1 (19%)	IL′CT, ILCT, ML′CT, MLCT
			H-2→L+1 (37%)	IL′CT, ILCT, L′LCT
			HOMO→L+3 (14%)	MLCT, ILCT
$S_0 \rightarrow S_{13}$	0.2461	277	H-5→LUMO (22%)	IL′CT, L′LCT
			H-3→L+1 (19%)	IL′CT, ILCT, ML′CT, MLCT
			HOMO→L+2 (22%)	ML′CT, LL′CT, IL′CT
$S_0 \rightarrow S_{18}$	0.2262	261	H-4→L+1 (10%)	MLCT, ML′CT
			H-3→L+3 (35%)	MLCT, ILCT, L′LCT
			H-2→L+3 (28%)	ML′CT, LL′CT, IL′CT
$S_0 \rightarrow S_{30}$	0.3414	242	H-5→L+1 (29%)	IL′CT, L′LCT, ILCT
			H-4→L+2 (20%)	ML′CT, LL′CT
			H-3→L+2 (15%)	ML′CT, IL′CT, LL′CT
			HOMO→L+4 (12%)	ML′CT, IL′CT, LL′CT

Table S9. Wavelengths and corresponding nature of transitions for the complex **3** where M = Pt, L = ppy and L′ = CN-tBu.

Excited state	Oscillator strength	Calculated λ (nm)	Transitions (Major Contribution)	Assignment
$S_0 \rightarrow S_1$	0.0419	354	HOMO→LUMO (95%)	MLCT, ILCT
$S_0 \rightarrow S_3$	0.1127	317	H-3→LUMO (11%)	MLCT, ILCT
			H-2→LUMO (82%)	MLCT, ILCT
$S_0 \rightarrow S_5$	0.2234	284	H-3→LUMO (29%)	MLCT, ILCT
			HOMO→L+1 (58%)	MLCT, ILCT
$S_0 \rightarrow S_8$	0.0835	268	H-2→L+1 (72%)	MLCT, ILCT
			HOMO→L+2 (17%)	ML′CT, LL′CT, ILCT
$S_0 \rightarrow S_{11}$	0.3854	259	H-2→L+1 (11%)	MLCT, ILCT
			H-2→L+2 (18%)	MLCT, ILCT, ML′CT
			HOMO→L+2 (50%)	ML′CT, LL′CT, ILCT
$S_0 \rightarrow S_{12}$	0.0937	253	H-3→L+1 (41%)	MLCT, ILCT
			H-3→L+2 (13%)	ILCT, ML′CT, LL′CT
			H-2→L+2 (26%)	MLCT, ILCT, ML′CT
			HOMO→L+2 (12%)	ML′CT, LL′CT, ILCT
$S_0 \rightarrow S_{13}$	0.1683	251	H-6→LUMO (14%)	MLCT, ILCT
			H-3→L+1 (42%)	MLCT, ILCT
			H-2→L+2 (19%)	MLCT, ILCT, ML′CT

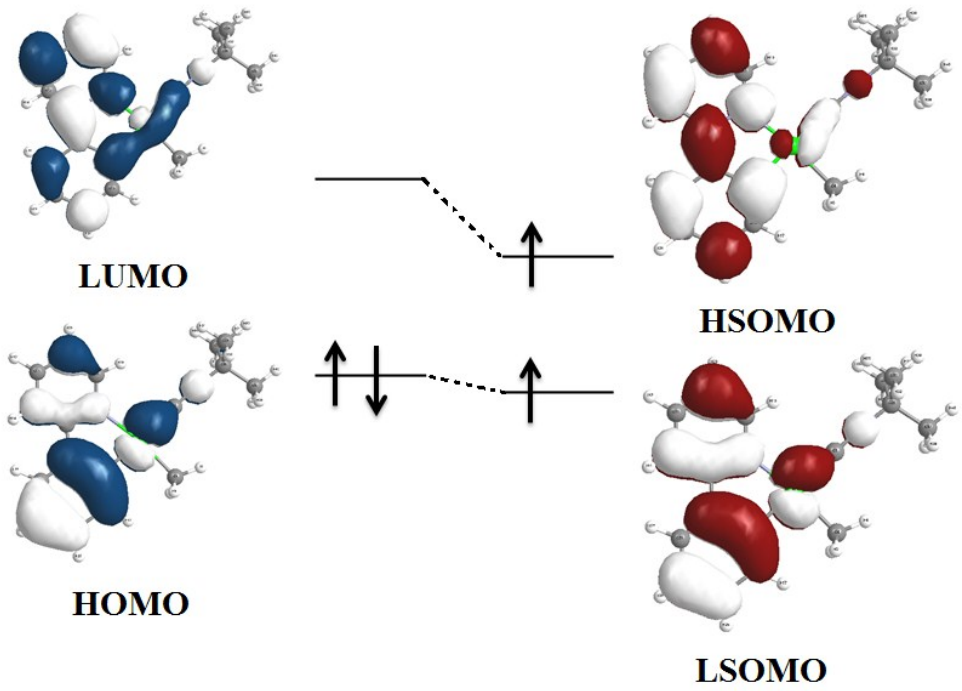

Figure S24. Molecular orbital plots for the computed S_0 (left) and T_1 (right) states of complex **3**.

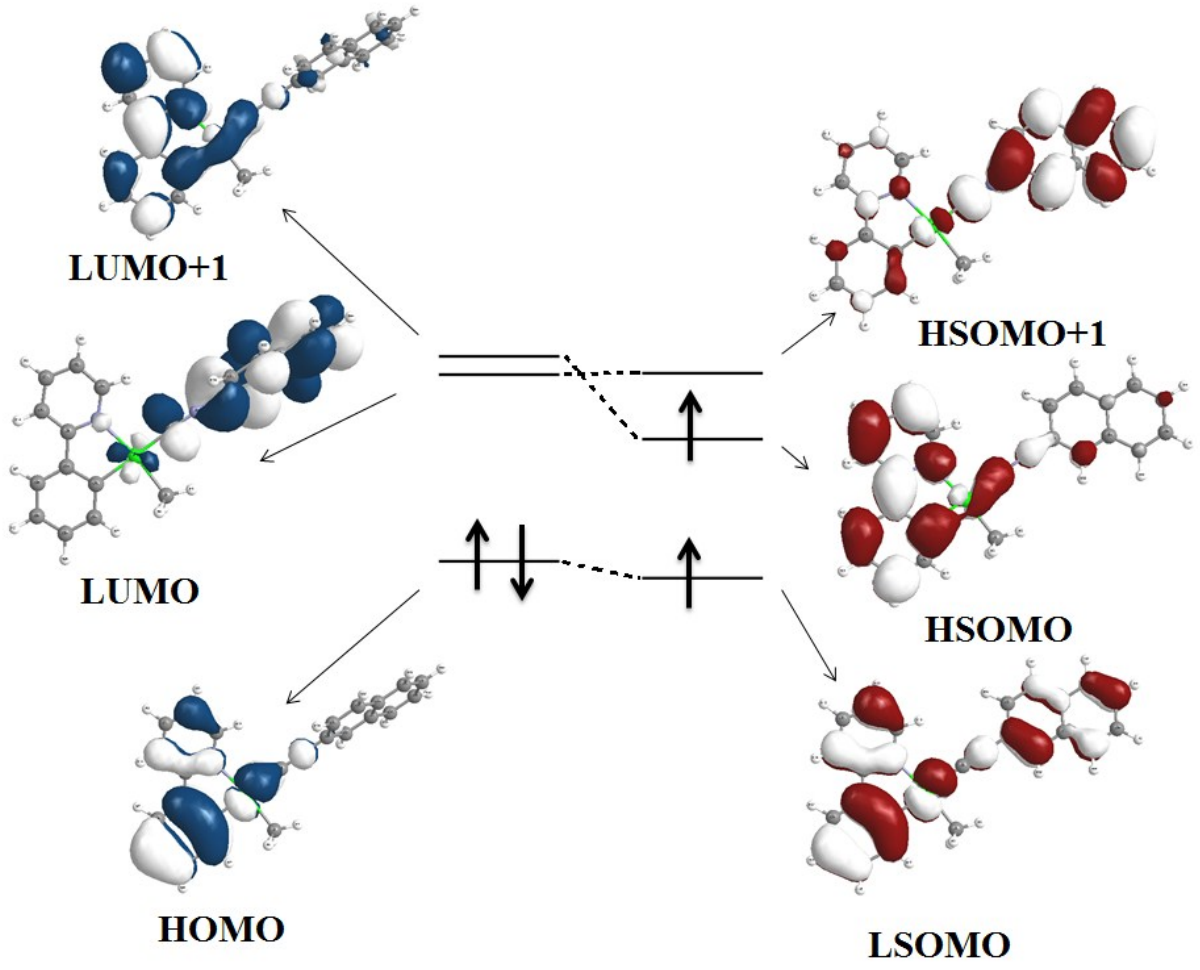

Figure S25. Molecular orbital plots for the computed S_0 (left) and T_1 (right) states of complex **2**.

Table S10. Crystallographic and structure refinement data for **1** and **3**.

	1	**3**
Empirical formula	$C_{20}H_{18}N_2Pt$	$C_{17}H_{20}N_2Pt$
Formula weight	481.44	447.43
Temperature	298(2) K	293(2) K
Wavelength	0.71073 Å	0.71073 Å
Crystal system, space group	Monoclinic, *C2/c*	Orthorhombic, *P212121*
Unit cell dimensions	a = 21.311(4)Å	a = 9.3461(19) Å
	α= 90°	α= 90°
	b = 12.257(3) Å	b = 10.106(2) Å
	β= 128.40(3)°	β= 90°
	c = 16.659(3) Å	c = 17.704(4) Å
	γ = 90°	γ = 90°
Volume	3410.2(19) $Å^3$	1672.2(6) $Å^3$
Z, Calculated density	8, 1.876 Mg/m^3	4, 1.777 Mg/m^3
Absorption coefficient	8.230 mm^{-1}	8.383 mm^{-1}
F(000)	1840	856
θ range for data collection	2.08 to 24.99°	2.30 to 25.00°
Limiting indices	-25<=h<=24,	-9<=h<=11,
	-14<=k<=14,	-10<=k<=12,
	-19<=l<=19	-19<=l<=21
Reflections collected	9010	5278
Completeness to θ	= 24.99, 99.9 %	= 25.00, 100.0 %
Independent reflections	3001 [R(int) = 0.0814]	2936 [R(int) = 0.1076]
Refinement method	Full-matrix least-squares on F^2	Full-matrix least-squares on F^2
Data / restraints / parameters	3001 / 0 / 209	2936 / 0 / 173
Goodness-of-fit on F^2	0.878	0.949
Final R indices [I>2sigma(I)]	R1 = 0.0375, wR2 = 0.0616	R1 = 0.0496, wR2 = 0.1102
R indices (all data)	R1 = 0.0736, wR2 = 0.0678	R1 = 0.0633, wR2 = 0.1141
Extinction coefficient	n/a	n/a
Largest diff. peak and hole	0.832 and -1.077 e.$Å^{-3}$	2.159 and -1.502 e. $Å^3$
CCDC No.	1569649	1569650